LINLI ZHANG

PROPRIÉTÉS ELECTROCHIMIQUES D'UN COMPOSITE EN POLYLACTIDE/POLYPYRROLE ET SYNTHÈSE ELECTROCHIMIQUE D'UNE MEMBRANE EN POLYPYRROLE

ELECTROCHEMICAL PROPERTIES OF A POLYLACTIDE/ POLYPYRROLE COMPOSITE AND ELECTROCHEMICAL SYNTHESIS OF A FREE-STANDING POLYPYRROLE MEMBRANE

Mémoire présenté

A la Faculté des études supérieures de l'Université Laval

Dans le cadre du programme de maîtrise en médecine expérimentale

pour l'obtention du grade de Maître ès sciences (M.Sc.)

FACULTÉ DE MÉDECINE

UNIVERSITÉ LAVAL

QUÉBEC

2010

ACKNOWLEDGMENTS

I first wish to express my sincere and deepest gratitude to my supervisor Dr. Ze Zhang for providing me with this exceptional opportunity to continue my studies toward a Master's degree, and for leading me into the attractive field of conductive polymers. The research project has expanded my academic background and enriched my research experience. I truly appreciated his patience and suggestions regarding my courses and research.

I also wish to acknowledge my colleague Shiyun Meng for providing me with experimental materials and professional advice for my research.

I am also grateful to Stephane Turgeon and Pascale Chevallier for their technical assistance on the XPS analyses.

Finally, my heartfelt thanks to my family and my partner Liu Jia for their unwavering encouragement and support during my studies abroad over two and a half years. Their love and support gave me the confidence to complete my studies.

RÉSUMÉ

Les polymères conducteurs sont fréquemment utilisés en génie biomédical pour la transmission de signaux électriques. Les objectifs de ce mémoire étaient d'évaluer l'électroactivité d'un composite de polymère conducteur, et d'explorer une nouvelle technique de synthèse d'une membrane mince à partir de ce polymère conducteur.

L'effet de l'héparine comme dopant polyanionique sur l'électroactivité du composite a été évaluée par voltammétrie cyclique (CV) et comparée à l'effet des anions de chlore. Le composite dopé par héparine a été trouvé électriquement actif avec une stabilité améliorée de façon significative. Ces résultats confirment le potentiel de l'utilisation de ces composites conducteurs pour des applications biomédicales à long terme.

Les membranes minces des polymères conducteurs sont généralement synthétisées par polymérisation électrochimique à la surface de l'électrode. Des membranes souples et autoportants de polypyrrole (PPy) et le copolymère de pyrrole et 1-(2-carboxyéthyl)pyrrole (PPy/PPyCOOH) par électropolymérisation à l'interface air/liquide (électrolyte) ont été produites dans le cadre de ce mémoire. Ces membranes ont démontré une électroactivité stable pour un minimum de 200 balayages de CV. La membrane PPy/PPyCOOH a également démontré une importante activité d'oxydoréduction. Ces membranes peuvent être utilisées dans des biosenseurs ou des piles souples.

SUMMARY

Conductive polymers are increasingly being used in biomedical engineering to mediate electrical signals. The objectives of this thesis were to evaluate the electroactivity of a conductive polymer composite and to explore a new approach to synthesize free-standing conductive polymer film.

The effect of polyanionic dopant heparin (HE) on the electroactivity of the composite was studied using cyclic voltammetry (CV) and was compared with the effect of chlorine anions. Heparin-doped composite was found to be electrically active with significantly improved stability. These findings support the potential of using conductive composite for long-term biomedical applications.

Conductive polymer thin film is typically synthesized through electrochemical polymerization on the surface of a working electrode. This thesis successfully generated flexible free-standing films of polypyrrole (PPy) and the copolymer of pyrrole and 1-(2-carboxyethyl)pyrrole (PPy/PPyCOOH) through electropolymerization at the air/liquid (electrolyte) interface. These films showed stable electroactivity for at least 200 CV scans. The PPy/PPyCOOH films showed significant redox activity. These films may be used in biosensors or flexible batteries.

TABLE OF CONTENTS

LIST OF TABLES

CHAPTER II

1. Surface elemental composition and the C_{1s} components of the conductive membranes before and after cyclic voltammetric characterization.

CHAPTER III

1. Surface chemistry of the free-standing PPy films before and after CV scan, and the compared surface chemistry of the PPy/PPyCOOH and the PPy deposited on the Pt surface, as measured by XPS.

LIST OF FIGURES

CHAPTER II

between 150 and 1000 scans for both membranes, and between 500 and 1000 scans for the PLLA/PPy/HE membrane.

7. The change of charge transfer with the increasing number of scans, showing a pattern similar to that of the anodic and cathodic currents. Dash lines represent the linear regression between 150 and 1000 scans for both membranes, and between 500 and 1000 scans for the PLLA/PPy/HE membrane.

8. Scanning electron microscope photomicrographs of the PLLA/PPy (95:5) composite membranes before (A, C) and after (B, D) 1000 CV scans.

9. ATR-FTIR spectra of the composite membranes before (B) and after (A) 1000 CV scans and spectra of the reference materials.

CHAPTER III

1. Macroscopic images of the free-standing PPy film (A), the PPy deposited on the Pt plate (B), the very small PPy film on the Pt wire, and the free-standing PPy/PPyCOOH film on the Pt plate (D), showing the significantly larger film size compared to that synthesized according to literature #6.

2. CV scans of the free-standing PPy film generated electrochemically at the air/liquid interface, showing the film to be electrically active, and the unclear redox behaviour of the PPy film.

3. CV scans of the free-standing PPy/PPyCOOH film generated electrochemically at the air/liquid interface, showing the clear redox behaviour of the copolymer film.

4. CV scans of the regular PPy deposited directly on the Pt electrode, showing the typical redox behaviour and high electroactivity.

5. CV scans of the regular PPy/PPyCOOH deposited directly on the Pt electrode, showing the typical redox behaviour and high electroactivity.

6. ATR-FTIR spectra of the free-standing PPy film, the regular PPy, and the PPy/PPyCOOH copolymer film, showing the oxidation of the PPy film and the presence of the PPyCOOH in the PPy/PPyCOOH copolymer.

7. Scanning electron microscope photomicrographs of the regular PPy deposited on the working electrode (A and B), showing the typical "cauliflower" morphology of PPy. The PPy film deposited at the air/liquid interface (C and D) displayed a completely different morphology.

CHAPTER I

INTRODUTION

1.1   Motivation

Conductive polymers can be used as an interface to transfer electrical signals between external electrical control units and biological systems such as cells. These signals may represent the electrical activity generated by nerve cells, or the external electrical potential used to stimulate smooth muscle cells. Conductive biodegradable composite made of conducting polypyrrole (PPy) and biodegradable poly(L,L-lactide) (PLLA) has been developed by Dr. Zhang's group. This composite is used as a semi-conducting substrate to deliver electrical stimulation to the cells cultured on it. In all of the previous research, this composite substrate was integrated into a closed electrical circuit rather than being used as an electrode. In fact, this conductive composite may also be used as an organic electrode. Electrodes have important biomedical applications such as neural prostheses and biosensors. Compared to the metal electrode, an organic biodegradable electrode provides the advantage of temporary use without surgical explantation, tunable mechanical properties, and easy chemical modification. However, two critical properties of the conductive composite, namely, electroactivity and electrical stability when used as an electrode, have not been studied.

Conductive polymer thin film is usually electropolymerized on the surface of an electrode and is then peeled off. My preliminary experiment found that under specific electrochemical conditions, PPy forms a free-standing film at the air/liquid interface. This film is flexible and can be cut and rolled into a tube. This phenomenon thus provides an interesting alternative approach to generate thin and flexible conductive polymer films that are currently extensively explored for applications such as sensoring and light, flexible batteries. However, the conditions to form large films and their properties have not been studied.

2

1.2   Hypotheses

A. Conductive biodegradable PLLA/PPy composite membrane may be used as an organic electrode.

B. Free-standing conducting film may be electrochemically synthesized at the air/liquid interface.

.

1.3   Objectives

A. Investigate the electroactivity and stability of the PLLA/PPy composite membrane using cyclic voltammetry.

B. Electrochemically synthesize a free-standing conducting film based on pyrrole and 1-(2-carboxyethyl)pyrrole.

1.4   Literature review

PPy is one of the most studied conductive polymers in the world because of its high conductivity, environmental stability, and easy synthesis. Because of its highly conjugated and cross-linked polymer chains, PPy is also insoluble and non-fusible. The electrical conductivity and mechanical properties of PPy are closely related to its polymerization conditions such as electrolyte anions, solvents, pH, and temperature. When PPy is oxidized and doped by anions, its conductivity can be as high as 10^2-10^3 S/cm, with a tensile strength up to 50-100 MPa (1). PPy is synthesized through the oxidation of either pyrrole or substituted pyrrole monomers. Polymerization can normally be performed using two techniques: electrochemistry and wet chemistry. Through the electrochemical approach, PPy is formed by the oxidation of pyrrole at an oxidative electrical potential on the surface of a suitable anode. Upon application of positive potential to the anode, pyrrole molecules near the anode are oxidized and deposited on the anode as PPy. Chemical polymerization takes place in a solution through the action of a soluble chemical oxidant. These various polymerization methods produce PPy in various forms; chemical oxidation generally

3

produces insoluble black powders, and electrochemical synthesis forms PPy coated on the surface of a working electrode. The chemical structure of pyrrole and PPy is shown in Figures 1-1 and 1-2.
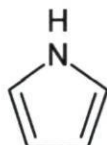
Figure 1-1. Pyrrole monomer　　　　Figure 1-2. "Ideal" polypyrrole structure
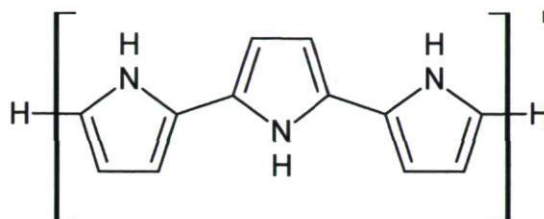
1.4.1 Discovery of PPy

The first PPy was reportedly produced in 1916 by oxidizing pyrrole with H_2O_2, which produced a kind of black powder then referred to as pyrrole black. Because this pyrrole black was not conductive and showed little potential for use, it was largely ignored. The electrochemical synthesis of PPy dates back to the early work of Dall'Ollio, who also obtained pyrrole black in aqueous sulfuric acid on a platinum electrode (2). It was not until 1979 that the electrochemical synthesis of PPy became a useful way to obtain highly conductive materials. Chemical and electrochemical synthesis methods have since been improved upon to optimize the physical and chemical properties of these materials (1).

1.4.2 Synthesis of PPy

As mentioned above, chemical and electrochemical polymerizations are the two main methods used for PPy synthesis. The primary advantage of the chemical method is the large production at low cost. The electrochemical method, on the other hand, provides PPy with better conducting properties and *in situ* polymerization.

1.4.2.1 Electrochemical polymerization

Electrochemical polymerization is the most appropriate method to obtain high-conductivity PPy. In a three electrode system controlled by an electrochemical potentiostat, anodic current is applied through a working electrode to the solution containing an electrolyte and pyrrole monomers. When the voltage applied to the working electrode is higher than the oxidation potential of the pyrrole molecules, these molecules are oxidized and deposited on the working electrode (anode), forming PPy. The electrochemical polymerization of pyrrole is a fast and simple process; after only a few seconds (depending on the applied potential) following the beginning of anodic current, PPy begins to deposit on the electrode. The experimental requirements are easy to be satisfied because polymerization can be carried out in an aqueous solution at ambient pressure and temperature.

The polymerization reaction of PPy can be simplified as:
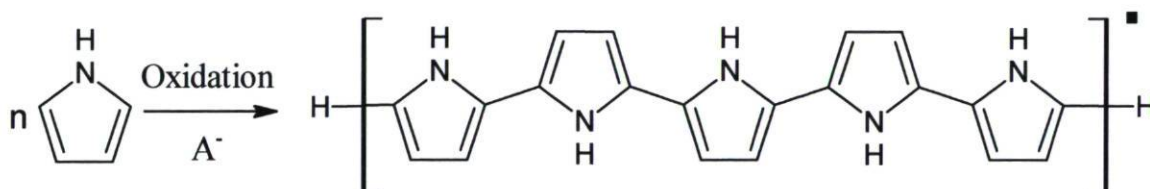
Figure 1-3. Polymerization reaction of PPy

A^- represents the counterions that electrostatically interact with the positively charged nitrogen on the pyrrole ring, thus maintaining the oxidative state of the PPy. In an "ideal" structure, counterions are presumed to be sandwiched between the planar pyrrole rings. However, because of the high degree of cross-link and branching at C_3 and C_4, PPy chains are distorted, making the ideal PPy structure difficult to obtain. Figure 1-4 illustrates the dynamic interactive nature of PPy when polymer synthesis is initiated (3):

The first step (monomer oxidation):
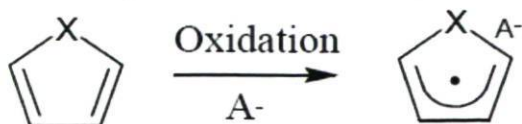
The dynamic structure of the oxidized monomers:
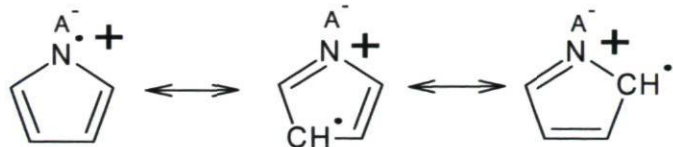
Step two, radical–radical coupling:

Step three, rapid deprotonation and subsequent oxidation:
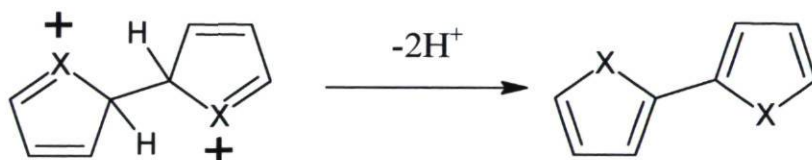
Polymerization is considered to proceed via a radical–radical coupling mechanism.
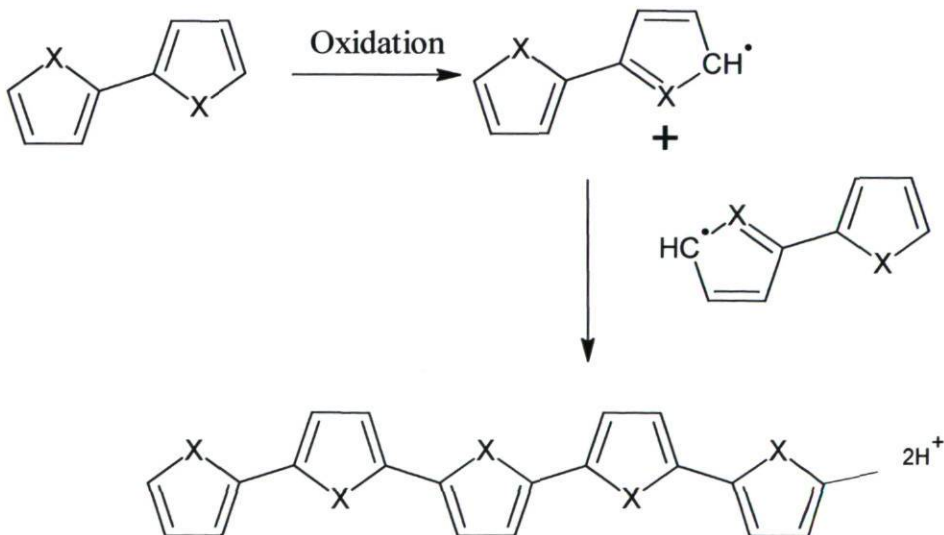
Figure 1-4. PPy polymerization process (3)

Chain growth continues until it exceeds a critical length and precipitates on the surface of the working electrode. Although knowledge regarding PPy has greatly developed, it remains unclear where the radical–radical coupling occurs and whether the continued chain growth occurs in the solution or on the electrode surface. We do know, however, that some polymerization occurs in the solution, and that the polymer molecules interact with the bare electrode or with the PPy-deposited electrode to produce the final structure. When the reaction begins, an initial layer of PPy is deposited on the anodic electrode and becomes a reactant, to which the remainder of the pyrrole monomers react. Studies have shown (4) that PPy polymerization occurs more readily at a lower potential on deposited PPy than on a bare electrode surface, i.e., 600 mV vs. 680 mV, respectively. Electrochemical conditions, electrode material, solvent, monomer, these are all important elements influencing PPy polymerization. For example, if the anode potential is too low, no precipitation occurs on the electrode, and if the solvent is nucleophilic (or contains dissolved oxygen), it will react with the free radical intermediates (5).

Polymerization rate is another important factor and is largely determined by the positive potential on the working electrode used to force monomers to oxidize. If the polymerization rate is too slow, only limited PPy deposition will occur, as the oxidized pyrrole monomers may leave the reaction zone near the electrode surface before reaching the critical size of deposition. On the other hand, there is an upper limit for the positive potential. An oxidation potential that is too high will result in the overoxidation of the PPy, meaning less conductive, inferior mechanical properties.

All of the afore-mentioned parameters also influence the overall reaction rate. For example, at the initial stage of polymerization, the type of electrode substrate influences reaction rate. Monomer concentration also plays a definitive role in that the concentration of pyrrole monomers may excessive when the reaction is initiated; however, due to the consumption of the monomers, a low monomer concentration may become the rate-limiting factor. Electrolyte stirring and temperature are also essential, as they control the

rate of transport of reactants and products to and from the electrochemical reaction zone. This in turn determines polymerization efficiency. Furthermore, hydrodynamics are crucial in determining the form of the produced PPy. For example, using a flow-through cell and under appropriate chemical conditions, stable colloidal dispersions rather than insoluble films may be produced (5).

1.4.2.1.1 Effect of electrochemical conditions

The electrochemical polymerization of PPy involves many experimental parameters (electrode, solvent, electrolyte, monomer, potential, pH of the solution, temperature) that all affect polymer synthesis.

1.4.2.1.1.1 Electrode

The electrode is a major component in PPy electropolymerization, particularly in the initial stage of reaction before it is coated by the PPy. The adsorption and easy oxidization of the monomers on the electrode are largely determined by the nature of the electrode material. Whether or not deposition occurs depends on the surface energy of the electrode and controls the hydrophobic/hydrophilic nature of the deposited polymer (5). While PPy is produced by and deposited on the electrode, the electrode itself should not oxidize. Thus inert substances, such as stainless steel, glassy carbon, gold, aluminum, and platinum, are often used. When a non-inert metal is used as the working electrode, the polymerization of PPy is interfered by the anodic oxidation. The rate of electron transfer subsequently declines as the reaction goes on. The size of the working electrode is yet another significant factor influencing electrosynthesis.

At cyclic voltammetry, the behaviour of the auxiliary electrode at anodic potential is also the key, as this electrode is also exposed to positive potentials. If the material used easily oxidizes, the release of metal ions into the solution can interfere with the

polymerization process at the anode. It is thus necessary to avoid these reactions occurring at the auxiliary electrode, including possible reactions with the solvent. The auxiliary electrode usually consists of electrochemically inert metals such as Pt wire.

1.4.2.1.1.2 Solvent

The solvent has an obvious influence on the polymer's properties during electropolymerization. It is not merely a reaction medium, but also an integral part of the polymerization. Solvents may also affect the conformational nature of the products, which is analogous to that observed with other macromolecules, such as proteins, that can fold in aqueous solution to protect their hydrophobic groups, yet unfold in more non-polar solvents to expose these same groups (5).

The solvent should be as pure as possible. Dissolved oxygen in solvent should be removed as much as possible, because it may react with radical intermediates and be reduced at the auxiliary electrode to form hydroxide during the polymerization process. Dissolved oxygen has a strong negative influence on the conductivity of PPy; thus, prior to reaction, purging the reaction solution with nitrogen gas for a period of time (for example, 10 minutes) is essential.

Obviously, the solvent must be able to dissolve both the monomers and the counterions at appropriate concentrations and be stable enough at the required electrical potential to avoid decomposition during the reaction. However, if the products of the solvent decomposition are innocuous, this solvent may be used as the polymerization medium. The interactions of the solvent with electrodes, monomers, and counterions must also be considered. The adsorption of monomers and counterions on electrodes depends on the solvent, thereby affecting the consequence of polymerization even before the reaction potential is applied. The nucleophilicity of solvent is also important because nucleophilic solvent reacts easily with free radical intermediates.

Aqueous solvent can be used in PPy synthesis and has been widely investigated. Water rather than organic solvent becomes a better choice because of its lower cost, ease of handling, safety, and minimum consequences to the environment. PPy films synthesized with aqueous solvent display physical properties and high conductivity that are similar to those of films produced with organic solvents.

1.4.2.1.1.3 Electrolyte

The supporting electrolyte has a strong effect on the properties of the synthesized conductive polymers. The principles to follow when selecting an electrolyte are the salt's solubility, its degree of dissociation in the appropriate solvent, the reactivity of the anions and the cations, and particularly the nucleophilicity of the anions (1). A wide range of anions can be used to synthesize PPy. Among these, sodium and potassium salts are commonly used, such as potassium-toluensulphonate, a good electrolyte that obtains high-conductivity PPy. Our experiment shows that electrochemically synthesized PPy displayed better stability and electroactivity when the electrolyte was potassium-toluensulphonate rather than sodium chloride.

Many researchers around the world have studied the electrolyte's performance during the electropolymerization process. The electrolyte not only influences the conductivity of the solution but also the rate of polymerization and the conductivity of the polypyrrole. The nature of the electrolyte salt employed can also strongly affect the polymer/solvent interactions and, most importantly, act as counterions.

It has been shown that the concentration of anionic electrolyte affects not only the amount of counterion incorporated into the polymer but also polymer structure and morphology. These morphological variations will further influence surface area and the subsequent rate of polymerization (6). Counterions should be stable during the reactions, (whether chemical or electrochemical polymerization). Otherwise, the unstable counterions

may interfere in the polymerization process. If the counterion's reaction potential is lower than the monomer oxidation potential, the potentiostatic method must be used to incorporate the polypyrrole. Moreover, in constant current method, the applied potentials are not constant and the counterions are preferentially oxidized.

The most productive counterions in terms of conductivity and mechanical properties appear to be sulfonated aromatics, and particularly para-toluenesulfonate (pTS) (7). It has been shown that benzene sulfonates induce a certain degree of crystallinity in conductive polymers, resulting in high conductivity (8). The high conductivity of the initially deposited polymer thus ensures an efficient polymerization process. Sulfonated aromatics, such as potassium-toluensulphonate, have also been shown in the literature (9) to display a surfactant-like behaviour, which stabilizes radicals and reduces attacks from the solvent, from oxygen, or from other nucleophiles.

The direct incorporation of biological molecules as the dopant into PPy is an attractive method in biomedical applications such as biosensors, neural prostheses, and novel cell culture surfaces. For example, heparin was electrochemically incorporated into PPy as the dopant by Wallace et al. (10) and chemically done by our group (11). Heparin is both a polyanion and an important glycosaminoglycan in cell membranes and extracellular matrix (11). The research undertaken by our group showed that conductive composite membranes containing heparin-doped PPy significantly increased electrical stability and cell adhesion compared to membranes without heparin-doped PPy.

1.4.2.1.1.4 Monomer

Pyrrole monomer, as showed here on the right, is a heterocyclic aromatic organic compound. Its structure consists of a five-membered ring. The formula is C_4H_5N, and the molecular weight is 67.09. Pyrrole has a
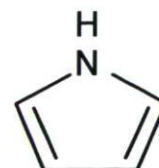
relatively high boiling point at 129-131°C and a low melting point at -23°C.

As we know, there are two positions on the pyrrole ring where substitution can take place, i.e., the N position and the 3 and/or 4 (β) position. Substitution at pyrrole nitrogen disturbs the conjugation of dislocated electrons and therefore lowers the electrical conductivity and mechanical properties of the resulting PPy (12). Alpha-substituted pyrrole monomers were reportedly not polymerized because these sites (2 and 5) are essential to polymerization (1). Substitution at the 3 and 4 (β) positions is thus usually preferred (13). Both pyrrole and substituted pyrrole monomers can be easily oxidized and then synthesized into polymers with good conductivity.

1.4.2.1.1.5 Temperature

Polymerization temperature has a strong influence on the polymerization, conductivity, redox properties, and mechanical characteristics of deposited PPy film. In general, PPy synthesized at lower temperatures such as 0°C displays a higher conductivity and better mechanical properties because of the relatively regular molecular structure. Synthesis at room temperature (ca. 20°C), however, is easy to operate and also produces good conductivity.

1.4.2.2 Chemical polymerization

Chemical polymerization is easier than electrochemical polymerization in terms of experimental parameters, with the obvious advantage that no expensive potentiostat and electrodes are required, nor are there any concerns regarding the type and quality of working electrode, electrolyte oxidation, or setup configuration, which all affect the outcome of an electrochemical process. While the range of counterions that may be incorporated into the PPy backbone during chemical polymerization are largely limited to anions associated with the oxidant, chemical polymerization remains the most practical

approach for processing purposes because it is easy to scale up and the products in the form of powders or colloidal dispersions are easy to use. For example, large-sized insulating fabrics can be easily coated with PPy. Chemical synthesis of PPy, in particular, has a significant advantage in that polymerization can be carried out in aqueous solution. A range of organic solvents, such as chloroform, may also be used, with only a consideration for the solubility of the pyrrole monomer and the oxidant.

1.4.3 Characterization

1.4.3.1 Cyclic voltammetry

Cyclic voltammetry (CV) is a potentiodynamic electrochemical measurement. In a voltammetry experiment, the working electrode potential is ramped linearly versus time, as in linear sweep voltammetry, although CV goes one step further. While linear sweep voltammetry ends when the potential reaches a predetermined value or set potential, when CV potential reaches a set potential, the working electrode potential inverses, sweeps back to the initial potential, and then sweeps back again. This cycling can take place multiple times during a single experiment (14). CV curves are recorded by plotting the current at the working electrode against the sweeping voltages. In a typical CV experiment, dissolved reactant and the formed conductive polymer are repeatedly oxidized and reduced in the reaction zone near the electrode and on the electrode surface, forced by the positive and negative potential on the electrode. For example, the potential of a working electrode begins at a particular voltage relative to a reference electrode such as an Ag/AgCl electrode. This electrode voltage is changed to a higher or lower voltage at a linear rate, and finally the voltage is changed back to the original value at the same linear rate. The redox reaction or the transfer of electrons between the reactant and the electrode takes place when the surface of the electrode becomes sufficiently negative (reduction takes place) or positive (oxidation takes place). The solution may obtain electrons from the electrode surface or transfer electrons to the electrode.

In a CV experiment, potential scans linearly versus time at a fixed rate, such as, for example, a scanning rate 50 mV/s. The potential is measured between the reference electrode and the working electrode and the current is measured between the working electrode and the auxiliary electrode. Data are plotted as current (I) versus potential (E). As shown in Figure 1 (Chapter II), the forward scan generates an oxidation peak where the current reaches a maximum as the potential sweeps to the top of the oxidation peak. The oxidation current then drops while the potential sweeps to the switch point, after which time the potential ramps in reverse to the reduction potential of PPy where a reduction peak occurs and then falls off to the end point (15).

A CV system normally requires a three-electrode setup. One of the electrodes is a reference electrode, which in this experiment was an Ag/AgCl electrode. The auxiliary electrode, a Pt wire also used in this study, provides a current drain to the working electrode, leaving the current to the reference electrode basically unchanged (16). Common materials for the working electrode include glassy carbon, platinum, and gold. As this work focused on characterizing the electrical stability and activity of the conductive polymer composite, PPy composite membranes were used as the working electrode.

1.4.3.2 Scanning electron microscopy

The scanning electron microscope (SEM) takes topographic images of a surface by scanning it line-by-line with a high-energy beam of electrons. Characteristic steric topography by SEM is generated by the secondary electrons as a result of interactions between the scanning electron beams (primary electrons) and the target surface. SEM is one of the most widely used analytical tools in surface analysis because it provides surface topographic images with a resolution as high as a few nanometers.

In addition to secondary electrons, the interaction of scanning electrons with the surface also generates back scattering electrons (BSE), characteristic X-rays, light,

transmitted electrons, and specimen current (17). A well equipped SEM may have more than one detector to not only measure surface topography but also surface elemental composition and distributions using BSE and characteristic X-ray.

SEM has been widely used in conductive polymer studies because many surface characteristics of conductive polymers are related to synthetic conditions and material properties. For example, PPy morphology is significantly affected by the nature of the dopant and by electrochemical polymerization conditions.

1.4.3.3 X-ray photoelectron spectroscopy

X-ray photoelectron spectroscopy (XPS), also known as electron spectroscopy for chemical analysis (ESCA), is the most valuable analytical tool for surface chemistry. The XPS machine, which is expensive and less available than most other analytical tools, provides quantitative information on surface elemental composition and surface molecular structures that may differ from the total elemental composition or bulk molecular structures. Surface property is critical in many circumstances (18). XPS is a real surface analysis technique capable of sampling a depth of approximately 10-100 angstroms (19).

In XPS analysis, atoms on a sample surface are irradiated by accelerated X-ray, causing the emission of photoelectrons from the sample surface. An electron energy analyzer captures these photoelectrons and determines their intensity and dynamic energy. The binding energy of the photoelectrons, which is characteristic for each element and is sensitive to the chemical environment surrounding this element, can then be calculated. The information obtained from XPS spectra includes the surface element content, the chemical state of the element, and the depth profile of surface elements (20). The main components of an XPS system include the X-ray source, an ultra-high vacuum (UHV) a stainless steel chamber with UHV pumps, an electron collection lens, an electron energy analyzer, Mu-metal magnetic field shielding, an electron detector system, a moderate

vacuum sample introduction chamber, sample mounts and sample stage, and a set of stage manipulators (18). The typical XPS spectrum is a graph of the number of electrons detected versus the binding energy of the electrons detected (20). Every element produces a characteristic set of XPS peaks at specific binding energy values. These peaks provide information to identify the elements existing in or on the surface of the material.

1.4.3.4 Infrared spectroscopy

Infrared spectroscopy (IR) deals with the molecular vibration in the infrared region of the electromagnetic spectrum. It is one of the most widely used analytical tools to identify chemical compounds and to investigate chemical structures. IR provides specific information on the nature of chemical bonds in molecules and on the interactions between molecules. It is very useful for analyzing organic materials. Chemical bonds naturally vibrate at characteristic frequencies. Upon exposure to infrared radiation, the chemical bonds absorb the radiation at these specific frequencies that match their vibration modes. Measuring the radiation absorption as a function of frequency produces a spectrum that can be used to identify functional groups and compounds (21).

1.4.4 Electrical conductivity of PPy

The most important property of conductive polymers is their electrical conductivity. In contrast to metals, which are rich in free electrons, the most widely accepted theory of conductivity in conductive polymers involves polarons and bipolarons as charge carriers, charge transport along the conjugated polymer chains, and a hopping of the charge carriers between polymer chains (22). Conducting polymers are semiconductors; their conductivity is also explained in terms of solid physics in which a semiconductor has a filled valence band and an empty conduction band. These bands are separated by an energy gap (23). Doping creates new bands in the energy gap, making it possible for the electrons to move to these new bands and increasing the conductivity of the materials (24).

The transport of charge carriers (electricity) occurs through the movement of the charge carriers along segments of conjugated polymer chain and the hopping of these carriers from chain to chain. The number of these charge carriers contained in a material and their relative mobility controls the bulk electrical conductivity (24). The electrical conductivity of PPy was determined by two important factors, the number of carriers and the charge carrier mobility. Charge carrier density is determined by the doping level, with a high doping level corresponding to high conductivity. Temperature is another factor influencing conductivity, because when temperature declines, so does the conductivity. In contrast, metal conductivity increases with decreasing temperature. The electrical conductivity of PPy is thus strongly influenced by several polymerization factors, including electrolyte, counterion, doping level, current density, temperature, solvent, and electrode.

The electrical conductivity of conductive polymers (including PPy) decreases over time because of ageing which is the most common phenomenon for all polymer materials. For conductive polymers, age-related conductivity deterioration is caused primarily by dedoping and by oxygen reaction.

1.4.5 Electroactivity of PPy

In the realm of biomedical applications, the electroactivity of PPy, one of its most important properties, is characterized by the ion exchange between conductive polymer and the surrounding environment (such as culture medium and body fluid) and is driven by the electrical potential applied to the conductive polymer. Because it is a unique example of redox reaction, the electroactivity of PPy and other conductive polymers is accompanied by electron and dopant transport within the material (25). Due to its high electroactivity, PPy has been widely studied for many applications such as biosensors, drug delivery, artificial muscle, separation devices, and rechargeable batteries, among others.

The reduction-oxidation processes of PPy involve a change in resistance and an ion exchange, which is very different from other redox systems in electrochemistry in which only electrons are involved during these two processes (24). For example, when reduction potential is applied to PPy, the anionic counterions are expelled out of the pyrrole ring, resulting in the loss of electrical conductivity. On the other hand, PPy oxidation is accompanied by anion intake and the recovery of conductivity. Potential-driven ion exchange thus becomes the basis for electrically stimulated drug delivery. Ion exchange that alters the conductivity then becomes the basis for biosensing. A large amount of ion exchange also alters the volume of the conductive polymer, thus the basis for electrically stimulated mechanical deformation which is the premise of conductive polymer-based artificial muscles.

The overall electroneutrality of PPy at reduction is maintained by either the expulsion of the anionic counterions or the incorporation of cations from the environment (26). At oxidation, PPy units have positive charges that are balanced by the anionic counterions from the dopant, showing this general electroneutrality. At reduction, for example upon the action of a sufficiently negative potential, pyrrole nitrogen will lose its positive charge and become neutral, resulting in the expulsion of the anions from PPy, a process called dedoping. When counterions are difficult to expel, such as when bulky dopant or self-doping is used, cations from the environment can be drawn into PPy to counterbalance (neutralize) the anions (27). A good example is the use of polyanions as the dopant. Due to their large size, polyanions become trapped within the PPy matrix, and perhaps more importantly, become entangled with the PPy chain. Consequently, this increases the stability and mechanical strength of the PPy (25). The extent to which anions leave during reduction or when cations are taken in depends on the nature of the counterions, the cations, the potential, and the solvent involved (28).

CV is often used to investigate these processes. In a typical CV curve, oxidation and reduction peaks can be obtained. The oxidation peak appears in the high potential

region accompanied by a positive current and the reduction peak takes place in the low potential region accompanied by a negative current. Because the release of counterions can be fairly accurately controlled, this mechanism offers interesting possibilities in the release of molecules of medical significance (29).

The electroactivity of PPy and other conductive polymers is strongly influenced by the nature of the dopant or the counterions. For example, greater electroactivity is achieved with sodium p-toluenesulfonate than with sodium chloride as the dopant. However, the basic molecular structure of conductive polymers is not affected by the nature of the dopant.

Oxidation potential is the most important factor affecting the electroactivity of PPy. When the supplied potential is not positive enough, the polymer chain fails to reach the ideal length, which in turn compromises conductivity and electroactivity. When the applied voltage is higher than the oxidation potential, overoxidation occurs, causing the breakdown of the conjugation structure and subsequent irreversible low electroactivity and conductivity. PPy is normally synthesized at a voltage of 0.6-0.7V relative to Ag/AgCl.

1.4.6 Environmental stability of PPy

Environmental stability is another essential property of conductive polymers. The stability of a material depends on two aspects: the material itself and the environment in which the material is used. To a different extent, oxygen, high temperature, and the presence of water are environmental factors that are harmful to conductive polymers. The decay of PPy conductivity is often related to oxidation that occurs in the presence of oxygen and is accelerated in the presence of water. Because of the solubility of most dopants in water, the presence of water is likely to cause the migration of dopant into the aqueous phase (dedoping) and the subsequent doping by oxygen atoms. High temperature favors the evaporation of small counterions such as chlorine anions.

The nature of conductive polymer also affects its stability. As we know, the oxidation potential of PPy is lower than that of most other conductive polymers (such as polythiophene), rendering it more vulnerable to oxygen. The conductivity of a conducting polymer tends to degrade over time even in dry and oxygen-free environments. This is likely due to the irreversible chemical reaction between the polymer's charged sites and either the dopant counterions or the π-system of the adjacent neutral chain, which produces a sp3 carbon that breaks the conjugation (30). Material instability may also occur through a thermally driven mechanism that causes the polymer to lose its dopant. This happens when the charge sites become unstable due to conformational changes in the polymer backbone (31).

Undoped PPy reacts easily with oxygen to generate a material with poor conductivity. Compared to the oxidized state, the reduced PPy is unstable in the presence of oxygen and water; the conductivity of oxidized PPy is fairly stable if oxygen and humidity are kept away. One study reported that oxygen adsorption onto the surface of conductive polymer and its diffusion inside limited the steps incorporating O_2 into the polymer, thereby blocking conducting pathways (32). The present study tested the stability of the PPy composite in an aqueous environment, as this composite is designed for biomedical applications that often involve an aqueous medium.

Conductivity stability is also affected by the nature of the dopant. For example, PPy displays greater stability and electroactivity when doped with p-toluenesulfonate (redundant) because small counterions such as chlorine anions can easily migrate into the solution and evaporate at high temperatures. The electrical stability of PPy is related to its ability to retain negative counterions. PPy can be switched to oxidized (conducting) or neutral (insulating) state accompanied by inward/outward-moving counterions (33). Thus the most important method to increase the electrical stability of PPy is to strengthen its interaction with counterions. Heparin used in our current work is a polyanion of high molecular weight whose strong interaction with PPy through multiple electrostatic

interactions and molecular entanglement is expected to increase the stability of heparin-doped PPy under aqueous conditions.

REFERENCES

1. J. Rodriguez, Polypyrrole: from basic research to technological application, in "Handbook of Organic Conductive Molecules and Polymers", Ed. H.S. Nalwa, John Wiley & Sons, Toronto, 1997; 415-460.

2. A. Dall'Olio, Y. Dascola, V. Varacca, V. Bocchi. J. Comptes. Rendus. 1968; C267: 433.

3. R. John, G. Wallace. The use of microelectrodes to probe the electropolymerization mechanism of heterocyclic conducting polymers. J. Electroanal. Chem. 1991; 306: 157-67.

4. S. Asavapiriyanont, G. Chandler, G. Gunawardena, D. Pletcher. The electrodeposition of polypyrrole films from aqueous solutions. J. Electroanal. Chem. 1984; 177: 229-44.

5. Gordon G. Wallace, Assembly of polypyrroles, in "Conductive Electroactive Polymers", 3rd Edition, CRC Press, New York, 2009; p.59-96.

6. Y. Shen, J. Qiu, R. Qian. Structure and amounts of counter ions in polypyrrole films prepared from aqueous solutions of sodium tosylate. J. Makromol. Chem. 1987; 188: 2041-5.

7. M. Salmon, A. Diaz, A. Logan, M. Krounbi, J. Bargon. Chemical modification of conducting polypyrrole films. J. Mol. Cryst. Liq. Cryst.1982; 83: 1297-308.

8. M. Kiani, N. Bhatt, F. Davies, G. Mitchell. Highly anisotropic electrically conducting films based on polypyrrole. J. Polym. 1992; 33: 4113-20.

9. M. Kiani, G. Mitchell. The role of the counter-ion in the preparation of polypyrrole films with enhanced properties using a pulsed electrochemical potential. J. Synth. Met. 1992; 48: 203-18.

10. B. Garner, A. Georgevich, A. Hodgson, L. Liu, G. Wallace. Polypyrrole-heparin composites as stimulus-responsive substrates for endothelial cell growth. J. Biomed Mater Res. 1999; 44: 121–129.

11. S. Meng, .R. Mahmoud, G. Shi, Z. Zhang. Heparin dopant increases the electrical stability, cell adhesion, and growth of conducting polypyrrole/poly(L,L-lactide) composites. J. Biomed. Mater. Res. 2008; 87A: 332-344.

12. W. Price, G. Wallace, H. Zhao. Effect of the counterion employed during synthesis on the properties of polypyrrole membranes. J. Memb. Sci. 1994; 87: 47-56.

13. M. Imisides, R. John, P. Riley, G. Wallace. The use of electropolymerization to produce new sensing surfaces: a review emphasizing electrodeposition of heteroaromatic compounds. J. Electroanal. 1991; 3: 879-89.

14. A. Bard, L. Faulkner. Electrochemical Methods: Fundamentals and Applications. 2nd Edition, John Wiley & Sons, New York. 2000.

15. Cyclic Voltammetry using a LabVIEW-based Acquisition System. Feb. 06, 2004 revision.Online:
www.earlham.edu/~chem/chem341/c341_labs_web/cyclic_voltammetry.pdf

16. R. Nicholson, I. Shain. Theory of stationary electrode polarography: single scan and cyclic methods applied to reversible, irreversible, and kinetic systems. J. Chem. 1964; 36: 706-23.

17. G. Danilatos. Foundations of environmental scanning electron microscopy. J. Adv Electron Phys. 1988; 71: 110-192.

18. R. Antonella, E. Bernhard, D. Nicholas. XPS surface analysis: imaging and spectroscopy of metal and polymer surfaces. J. Spectrosc. Eur. 2004; 6: 14-19.

19. B.V. Crist. Annotated Handbooks of Monochromatic XPS Spectra, J. Surf. Anal. 1998; 4: 428-434.

20. B.V. Crist. Annotated Handbooks of Monochromatic XPS Spectra Volume 3, John Wiley & Sons, Toronto, 2004.

21. P. Hamm, M. Lim. Structure of the amide I band of peptides measured by femtosecond nonlinear-infrared spectroscopy. J. Phys. Chem. 1998; 102: 6123-6138.

22. J. Bredas. Bipolarons in doped conjugated polymers: a critical comparison between theoretical results and experimental data. J. Mol. Cryst. Liq. Cryst. 1985; 118: 49-56.

23. J. Scott, J. Bredas, J. Kaufman, P. Peluger, K. Yakushi. Evidence for bipolarons in pyrrole polymers. J. Mol. Cryst. Liq. Cryst. 1985; 118: 163-170.

24. R. Ansari. Polypyrrole Conducting Electroactive Polymers: Synthesis and Stability Studies. E-J of Chem. 2006; 3: 186-201.

25. T. Shimidzu, A. Ohtani, T. Iyoda, K. Honda. Charge-controllable polypyrrole /polyelectrolyte composite membranes. Part II. Effect of incorporated anion size on the electrochemical oxidation-reduction process. J. Electroanal. Chem. 1987; 224:123-135.

26. J. Heinze, R. Bilger. Ion movements during redox switching of polypyrrole - experiment and simulation. J. Phys. Chem. 1993; 97: 502-510.

27. M. Depaoli, R. Peres. Properties of electrochemically synthesized polymer electrodes-- X. Study of polypyrrole/dodecylbenzene sulfonate. J. Electro.chem Acta. 1992; 37: 1173-1182.

28. G. Duffitt, P. Pickup. Permselectivity of polypyrrole in acetonitrile. J. Phys. Chem. 1991; 95: 9634-9635.

29. H. Naarmaan. Development of conductive polymers. J. Chem. Ind. 1991; 73: 401-408.

30. Y. Lam, J. Swingler, J. McBride. The contact resistance force relationship of an intrinsically conducting polymer interface. J. IEEE T Compon Pack T. 2006; 29: 294-302.

31. Y. Li, R. Qian. Stability of conducting polymers from the electrochemical point of view. Synth. Met. 1993; 53: 149-154.

32. T. Tansley, D. Maddison. Conductivity degradation in oxygen-aged polypyrrole. J. Appl. Phys. 1991; 69: 7711-13.

33. J. Kaufman, N. Colaneri, J. Scott, G. Street. Evolution of polaron states into bipolarons in polypyrrole. J. Phys Rev Lett. 1984; 53: 1005–1008.

CHAPTER II

ELECTROACTIVITY AND STABILITY OF THE POLYLACTIDE/POLYPYRROLE COMPOSITES

SUMMARY

Electrically conductive biodegradable composites are useful in biomedical engineering to mediate electrical interactions between cells and electrical components. Because conductive polymers are often subjected to progressive oxidative deterioration and dedoping, their electrical stability in aqueous environment is therefore critical. We used cyclic voltammetry to investigate the electroactivity and stability of conductive membranes made of only 5% conductive PPy particles blended with 95% insulating PLLA. During 1000 CV scans, the electroactivity of the composite membranes revealed a period of initial activation, followed by a relatively stable period and subsequent slow deterioration process. PPy membranes doped with heparin, a cell-adhesive polysaccharide and polyanion, displayed electrical stability superior to that of PPy membranes doped with chlorine anions. The latter, however, recorded a higher initial electroactivity during the first ca. 150 scans. XPS analysis showed that the deterioration of the electroactivity was likely due to the oxidation of the PPy. ATR-FTIR and SEM were also used to characterize the materials. The PLLA/PPy membranes were thus electroactive and maximum electroactivity was achieved through an activation process. The heparin-doped PPy composite was electrically stable and may thus be used for multiple long-term electrical stimulations.

INTRODUCTION

In recent years, conductive polymers, and in particular polypyrrole (PPy), have been studied with regard to the electrical stimulation of cellular functions. Research has revealed that the impact of electrical stimulation (ES) on cells may be similar to that of biological stimuli, such as growth factors (1), thus highlighting the significant potential of applied ES in tissue engineering and regenerative medicine.

It was reported that the presence of a steady and weak direct current electrical field in some biological systems affected cellular activities such as division, differentiation, migration, and the extension of motile processes (2). The efficacy of ES includes stimulating bone growth (3), enhancing wound healing (4), promoting early-stage nerve regeneration (5), affecting cellular migration (6), inhibiting endothelial cell proliferation (7,8), and directing cell division (9).

As one of the most important intrinsically conducting polymers, PPy acts as an interface between cells and tissues to deliver ES signals. PPy has been reported to support the adhesion and growth of a number of different cell types (10-12) and several studies have demonstrated its cell and tissue compatibility (13-17). We previously reported on a conductive composite made of 5% PPy particles and 95% biodegradable polylactide (PLLA) (18) and also demonstrated its in vitro cytocompatibility (18) and in vivo tissue compatibility (19). This material was able to mediate ES to modulate cellular activities (20).

To improve the electrical stability and cell adhesion of the PLLA/PPy composite, heparin (HE) was used as the dopant in synthesizing the PPy. Heparin is both a polyanion and an important glycosaminoglycan and is present on cell membranes and in extracellular

matrix. PLLA/PPy composite made of PPy particles doped with HE (21) was shown to display greater electrical stability than when doped with chlorine anions alone. In all of this previous research, the conductive composites were used as conductors integrated in a closed electrical circuit. In other important biomedical applications, such as neural prostheses or biosensors, conductive polymers are also used in the form of electrodes; however, the electroactivity and the stability of the conductive composites, critical parameters of conductive polymer electrodes, have yet to be studied.

The goal of this study was to investigate, for the first time, the electroactivity and stability of conductive biodegradable polymer composites in redox cycles. The significance is that using a conductive biodegradable composite as a stable electrode with no metal component provides more options to modify the electrode properties, such as mechanical properties, in order to suit the compliance of different tissues.

MATERIALS AND METHODS

Preparation of PLLA/PPy/HE and PLLA/PPy/ conductive membranes

Conductive composite membranes with heparin (PLLA/PPy/HE) and without heparin (PLLA/PPy) were prepared as reported previously (21). To synthesize PPy particles, a water-in-oil (chloroform) (3:7) emulsion system was prepared, in which the dispersed aqueous phase contained Fenton's reagent (oxidant) made by H_2O_2 and $FeCl_3$ (Laboratoire MAT, Québec, QC, Canada), as well as heparin (0.5% in total weight of PPy) (Sigma-Aldrich Canada Ltd., Oakville, ON, Canada) when necessary. Pyrrole monomers (98%, Aldrich Chemical Co., Milwaukee, WI, USA) were introduced dropwise to start polymerization, which took place under continuous stirring and nitrogen protection at room temperature for 24 h. Following polymerization, the PPy particles were precipitated with methanol and washed repeatedly with H_2O/methanol (1:1) to remove emulsifier and other impurities. The collected PPy was then used for subsequent experiments.

To prepare the conductive composite membranes, PPy particles were dispersed in a PLLA solution in chloroform with mechanical stirring for 24 h, followed by solution casting onto a polytetrafluoroethylene (PTFE) plate and drying to constant weight. The membranes were 0.5 mm in thickness with a weight ratio of 95:5 PLLA:PPy.

Electrochemical synthesis of PPy

As the reference materials, pure PPy was electrochemically synthesized on a platinum (Pt) working electrode in a three-electrode system controlled by an Epsilon potentiostat/galvanostat (BASi, West Lafayette, IN, USA), with Ag/AgCl as the reference and a Pt wire as the auxiliary electrode. Pyrrole monomers (0.1 mol/L) were dissolved in distilled water in which p-toluenesulfonate (0.1 mol/L, Sigma-Aldrich) was used as the electrolyte. PPy was polymerized potentiostatically at 1000 mV versus the Ag/AgCl. The reaction took 1000 seconds at room temperature. Following polymerization, black PPy was

found deposited on the surface of the Pt working electrode. The PPy-coated Pt electrodes were cleaned repeatedly in distilled water and dried in a vacuum oven prior to being subjected for cyclic voltammetry and XPS analysis.

Electrical characterization

To test the electroactivity and electrical stability of the composite membranes, the membranes were cut into 2.5 mm x 25 mm strips for use as the working electrode in a cyclic voltammetric experiment. An aqueous solution of *p*-toluenesulfonate (0.1 mol/L) was used as the electrolyte. Twenty millilitres of electrolyte in a cell vial was purged with nitrogen gas for 10 min prior to the experiment and was protected with nitrogen during the entire experiment. The selected experimental temperature was room temperature at approximately 20°C. The Epsilon potentiostat/galvanostat (BASi) was used to control the three-electrode system. One thousand cycles were run between -800 and 1200 mV at a scan rate of 50 mV/s. The PPy-coated Pt electrodes were also used as working electrodes and subjected to the same experimental conditions, which was then analyzed by XPS. Following thorough drying, the weight of the composite membrane electrodes was measured before and after the 1000 scans. Five experiments were performed for each type of composite membrane.

Surface analysis

Scanning electron microscopy (SEM)

The PLLA/PPy and PLLA/PPy/HE membranes with and without cyclic voltammetry testing were dried in a vacuum oven and were then sputter-coated with gold. The surface morphology of the specimens was observed under a JEOL JSM-35 scanning electron microscope (JEOL, Tokyo, Japan) at an accelerating voltage of 30 kV. At least two specimens from each membrane were observed.

X-ray photoelectron spectroscopy (XPS)

A Perkin Elmer PHI 5600 X-ray photoelectron spectroscope (XPS) (Perkin Elmer, Eden Prairie, MN, USA) was used to measure the surface elemental content (monochromatic aluminium source, 1486.6 eV) and the high resolution spectra (standard magnesium X-ray source, 1253.6 eV) of the functional groups of the specimens. The specimens included both the PLLA/PPy and PLLA/PPy/HE membranes with or without cyclic voltammetric testing. The emitted photoelectrons were collected at a 45° take-off angle and were analyzed with a hemispheric electron energy analyzer operating at two modes, namely, a pass energy of 187.9 eV for the survey scans and 5.85 eV for the high-resolution scans. The vacuum in the sample chamber was maintained at 10^{-10} torr during analysis. Curve fitting to the high-resolution spectra was performed using the software provided by the instrument manufacturer. At least three specimens from each membrane were analyzed.

Attenuated total internal reflection Fourier transform infrared spectroscopy (ATR-FTIR)

A Nicolet Magna-IR 550 spectrophotometer (Nicolet Instrument Inc., Madison, WI, USA) was used to analyze the surface chemistry of the composite membranes before and after the cyclic voltammetric analysis. The absorption spectrum was recorded by pressing the dry membrane specimens against the reflectance element and by averaging 150 scans at a resolution of four wavenumbers per centimetre. Curve fitting was performed using the software provided by the instrument manufacturer.

Statistical analysis

One-way ANOVA was used to analyze the statistical difference of the data. The difference between the control and test groups was considered significant when $p < 0.05$. Linear regression was performed on CV data using the software SigmaPlot 11.0.

RESULTS

Electrical characterization

Figure 1 presents the representative cycles of the first 100 scans of the PLLA/PPy membrane. As shown here, with the increase in cycles, both the anodic current and the integrated charge (area within the CV curve) increased continuously up to the 100th cycle which had the highest anodic current and integrated charge. Figure 2 shows the selected scanning curves from 150 to 1000, where the current and integrated charge was in constant decline. Similar results were observed for the PLLA/PPy/HE membranes (Fig. 3 and Fig.4), for which the highest anodic current and integrated charge appeared at the 150th cycle. It also appears that the decline of the anodic current was less significant for the PLLA/PPy/HE membrane than for the PLLA/PPy membrane. Apparent redox peaks appeared only after 100 to 200 scans at the position of ca. 400 mV and -300 mV, respectively. For the PLLA/PPy/HE membranes, the oxidation peak remained visible after 1000 scans. For the PLLA/PPy membranes, however, the redox peaks completely receded after 1000 scans.

To compare the electroactivity and resulting stability of the PLLA/PPy and PLLA/PPy/HE membranes, the highest anodic current (switch point at 1200 mV) and cathodic current (end point at -800 mV) of the representative cycles were normalized against their respective values of the 20th cycle and are plotted in Figure 5. The first 19 scans were ignored in this plot (also in Fig. 6 and Fig. 7) because their values were rather small. As is shown in Figure 5, while the increase in anodic current was high in the PLLA/PPy membrane up to 150 scans, reaching a ca. of 143% of the initial value, this gain diminished at the 550th scan and continuously dropped to a ca. of 76% of the initial value by the end of the experiment. For the PLLA/PPy/HE membrane, on the other hand, the peak anodic current reached a ca. of 126% in the first 150 scans and remained above 100% of the initial value with 105% recorded at the end of experiment. The cathodic current (Fig.

6) followed a similar trend, with the PLLA/PPy/HE membranes displaying the higher current over the long run as well as an overall better stability. The highest point was at the 150th scan, with 135% of the initial value, while the lowest point was 102% at the 1000th scan. For the PLLA/PPy membranes, the corresponding values were 139% at the 150th scan and 60% at the 1000th scan. Between 800 and 1000 scans, the differences between the two types of membranes were significant ($p < 0.05$).

Figure 7 presents the areas between the forward and backward scan curves of the PLLA/PPy and PLLA/PPy/HE membranes, thus indicating the integrated charge transfer. Similar to what is seen in Figure 5 and Figure 6, the areas increased continuously from the first scan up to the 100th scan, with a maximum increase of 157% and 163% for the PLLA/PPy and PLLA/PPy/HE membranes, respectively. The areas then gradually decreased between the 150th and 1000th scans. At this stage, the areas of the PLLA/PPy membrane showed a significant decrease, while the areas of the PLLA/PPy/HE membrane remained fairly stable. After 1000 scans, the change of the area compared to that in the first scan was -43% and 6% for the PLLA/PPy and PLLA/PPy/HE membranes, respectively.

Surface analysis

Scanning electron microscopy

Figure 8 shows the SEM images of the PLLA/PPy membranes before and after CV characterization. The goal was to investigate the morphological changes of the PPy particles before and after 1000 CV cycles. Figures 8A and 8C show the rough surface morphology of the membranes prior to CV cycling, revealing many irregular micro-domains formed by the aggregated PPy particles. Following 1000 CV cycles, it can be seen in Figures 8B and 8D that the membrane surface became relatively smooth, with the PPy particles seemingly submerged within the PLLA matrix. Cross-section observations of the membranes showed no significant difference before and after the CV characterization. The surface morphology and changes recorded by the PLLA/PPy/HE membranes were similar to those of the PLLA/PPy membranes (image not shown).

X-ray photoelectron spectroscopy

Table 1 presents the surface elemental composition and the deconvoluted C_{1s} and O_{1s} components of the conductive membranes before and after CV characterization. Prior to CV testing, the PLLA/PPy/HE and PLLA/PPy membranes showed a similar surface elemental composition, except for the significantly higher content of nitrogen on the PLLA/PPy/HE membranes ($p < 0.05$). The trace amount of chlorine was from the dopant chlorine anions in the PPy and also probably from solvent residue (chloroform). The presence of silicon was from contamination in the laboratory. Following CV characterization, the oxygen content increased 21% and 30% for the PLLA/PPy/HE and PLLA/PPy membranes, respectively, while their nitrogen content declined 48% and 8%, respectively. As for chlorine content, the PLLA/PPy/HE membranes showed constant values while the PLLA/PPy membranes showed a significant decrease of 41%. From the curve fitting results (Table 1), the O$\underline{C}$=O of both membranes significantly increased, with ca. 70% and 78% higher following the CV characterization.

Table 1 also presents the results of the PPy electrochemically synthesized on the Pt electrode. Compared to the composite membranes, the as-synthesized pure PPy recorded high nitrogen content from the pyrrole rings as well as a significant amount of oxygen. Following CV characterization, the oxygen content increased 48%, accompanied by an increase of C-O and OC=O.

ATR-FTIR

Figure 9 shows the infrared spectra of the PLLA/PPy and PLLA/PPy/HE composite membranes before and after CV characterization. Spectra of the pure PLLA, the PPy on the Pt electrode, and the heparin were also recorded as references. The spectra of both composite membranes before and after the CVs basically showed the same characteristics as those of the pure PLLA. The specific absorptions of PPy at 1546 cm^{-1} and of heparin at 1607 cm^{-1} were not visible.

Weight change

Following the CV test, the average weight of the PLLA/PPy/HE membranes increased by $0.26 \pm 0.08\%$. For the PLLA/PPy membrane, however, the average weight decreased by $0.24 \pm 0.11\%$. The difference was statistically significant ($p < 0.05$).

DISCUSSION

Through electrochemical characterizations, the results obtained in this work demonstrated that both the PLLA/PPy and PLLA/PPy/HE membranes are electrically active. Furthermore, the conductive membranes made by heparin-doped PPy particles had a super stability than the membranes made by PPy without heparin.

Unlike pure PPy, the conductive composite membranes used in this work displayed low electroactivity because only 5% of the membrane electrode was conducting PPy particles while the remaining 95% was insulating PLLA. The PPy particles exposed on the membrane surface were even more limited. This low PPy content and consequently low electroactivity were designed specifically to minimize the use of the non-biodegradable PPy.

One of the potential applications of conductive composites in tissue engineering may be scaffolding, in order to temporarily mediate ES to cells and tissues on a scaffold to promote tissue regeneration. Upon resorption of the biodegradable portion of the scaffold (PLLA in this case), only a minimum amount of PPy is ideally left (5% in this case) in the regenerated tissues, as PPy particles are "foreign materials" to the host. Luckily enough,

the ES of cells does not require high electroactivity or conductivity. Biological electrical field is usually in the range of microvolts (e.g., 10 to 200 mV), warranting the use of a very small amount of PPy in the scaffold. On the other hand, because of the hostile aqueous environment in cell cultures and in animal tissues, what is most critical is the stability of the electroactivity or the conductivity of the conductive scaffold, namely, how it is able to mediate multiple long-term ES (from days to weeks to months). As shown in Figures 1-2 and 3-4, the composite electrodes were electrically conductive between -800 and 1200 mV, which was enough to deliver biologically meaningful ES. The stability of the electroactivity of the composite electrode is the focus of the rest of the discussion.

The conductive membrane electrode recorded a dynamic process during the CV experiment. This dynamic process featured an initial activation period, followed by a stable period, and a final slow deterioration period (Figs. 1-2 and 3-4). During the initial activation period or the first 100 cycles, the membranes went from low electroactivity (defined by the maximum oxidation and reduction current and the charge transfer), with no redox characteristics, to an increasing electroactivity and subsequent visible redox peaks at ca. 400 mV and -300 mV versus Ag/AgCl. During ca. 100 and 150 cycles, the curves entered a rather stable phase, showing maximum electroactivity and redox characteristics. From 150 cycles on, i.e., the slow deterioration period, the electroactivity decreased over time and the redox characteristics diminished completely at the end of 1000 scans.

This unique electroactivity of the conductive composite membranes is the result of their material properties. With only 5% PPy particles embedded in the hydrophobic PLLA, the low initial electroactivity was predictable. The increase of electroactivity with further CV scans can be explained by the diffusion of the electrolyte into the composite (which caused more PPy particles to participate in the electrochemical process) and by the re-doping of the PPy particles by the toluenesulfonate anions at the high oxidative potential. Our data show a 0.26% weight increase of the PLLA/PPy/HE membranes after 1000 CV scans, indicating the possible uptake and retention of the toluenesulfonate molecules in this

composite membrane. If the weight increase was caused solely by the PPy-toluenesulfonate interaction, i.e., that 5% PPy particles caused 0.26% weight increase of the total membrane electrode, the weight increase of the PPy particles would have been 5.2%. The weak but clearly visible redox characteristics following the initial scans were likely the compounded effect of more PPy particle participation in the redox reactions, and the higher doping degree of the participating PPy particles following extensive CV cycling. The N_{1s} spectrum of the composite membrane, which otherwise may show the change of doping ratio at the different stages of CV cycling, was not detectable because of the low PPy content on the membrane surface.

The electroactivity of the PLLA/PPy/HE membranes was found to be more stable than that of the PLLA/PPy membranes. As is shown in Figure 5 and Figure 6, while the maximum oxidation (anodic) and reduction (cathodic) currents of the PLLA/PPy membranes were higher during the ca. first 150 scans, this high electroactivity lost its momentum gradually and proportionally with the increasing number of scans to ultimately decline to 76% of its initial value after 1000 scans. In contrast, the PLLA/PPy/HE membranes showed a very slow decrease of the maximum oxidation current and retained more than 100% of its original value at the end of the 1000 scans. This finding was confirmed by the maximum reduction current (Fig. 6) and by the total charge transfer (Fig. 7). In fact, following ca. 500 scans, the curves of the PLLA/PPy/HE membranes had almost flattened, showing a slope of -0.0126, while the curves of the PLLA/PPy membranes continuously decreased in the same manner, with a slope of -0.0732.

Based on a linear regression between 500 and 1000 scans (Fig. 5), the PLLA/PPy/HE membrane would retain 56% of its initial oxidation current after 10,000 scans, compared to a negative value by the PLLA/PPy membranes. The significance of using linear regression is to predict the lifetime of the composite membrane electrode. In this study, it showed that the PLLA/PPy/HE membrane is preferable for long-term ES experiments or applications. Following ca. 150 scans, the linear regression coefficient for all of the membranes was near or above 0.9, showing a predictable behaviour under a continuous redox process. HE, a polysaccharide of high molecular weight, is also a

38

polyanion. Its multiple electrostatic interactions with the oxidized PPy units and the physical entanglement with the PPy chains ensured the strong interactions between PPy and HE, thereby reducing the possibility of dedoping and the oxidation of PPy.

The mechanism of electroactivity deterioration was probably related to the progressive oxidation of the PPy. XPS data of all of the membranes recorded increased oxygen content, which was often accompanied by elevated C-O and O-C=O groups. This alone, however, does not prove the oxidation of the PPy, as PLLA contains both C-O and O-C=O groups. It is well known that incubation in aqueous environment induces the polar groups in a polymer's surface layer to orient toward the surface (19, 22). Thus the high oxygen content and oxygen-containing groups on the membrane surface does not necessarily signify PPy oxidation, particularly when considering the limited contribution of PPy to the total surface chemistry of the membrane. Nevertheless, the XPS data of the electrochemically synthesized pure PPy that underwent 1000 CV scans also revealed an increased oxygen content (48%) and an augmentation of C-O (45%) and O-C=O (31%) groups. This provides strong support to the possibility that the electroactivity deterioration of the composite membranes was related to PPy oxidation.

The subtle morphological alteration experienced by the composite membranes following 1000 CV scans is difficult to explain. While PLLA can be hydrolyzed, the 24 h (1000 scans) experiment most likely had no significant impact on surface texture. Considering the possibility of a re-orientation of PLLA surface polar groups and the altered membrane weight following the CV scans, the changes experienced (position, volume, aggregation) by the PPy particles may have occurred during the cycling as the particles "embedded" themselves deeper into the partially softened PLLA surface, thereby making the surface appear smoother than its initial state.

Under the hypothesis that PLLA measurable hydrolysis did not occur in only 24 h, the weight change of the composite membranes should be related to counterion uptake or loss. Because the CV scans ended at reduction, the weight loss of the PLLA/PPy membranes may have been caused by the loss of chlorine (original counterions) and toluenesulfonate (re-doped counterions) counterions. To explain the weight increase of the PLLA/PPy/HE membranes, we suggest that in the presence of the macromolecular HE, the aggregational structure of the PPy molecules was less compact compared to that of the PPy particles in the PLLA/PPy membrane. This ultimately made it easier for the toluenesulfonate molecules to penetrate and to interact with the PPy molecules during the oxidation scans and consequently they were less likely to be driven out at reduction.

CONCLUSIONS

The electroactivity and electrical stability of the PPy composite membranes were investigated by means of the cyclic voltammetry method. With only 5% PPy in the composite, the membranes were able to show biologically meaningful electroactivity and conductivity. To reach the maximum level of electroactivity, the composite membranes require an "activation" process that is controlled by the diffusion of the electrolyte and the scanning potential. The PLLA/PPy/HE membranes demonstrated superior electrical stability over the PLLA/PPy membranes and are expected to have a half life of 10,000 scans in aqueous environment.

ACKNOWLEDGMENTS

REFERENCES

1. D. Ateh, H. Navsaria, P. Vadgama. Polypyrrole-based conducting polymers and interactions with biological tissues. J. R. Soc. Interf. 2006; 22: 741–752.

2. C. McCaig, M. Zhao. Physiological electrical fields modify cell behavior. J. BioEssays. 1997; 19: 819–826.

3. L. Lavine, A. Grodzinsky. Electrical stimulation of repair of bone. J. Bone Joint Surg. Am. 1987; 69: 626–630.

4. R. Karba, D. Semrov, L. Vodovnik, H. Benko, R. Savrin. DC electrical stimulation for chronic wound healing enhancement, Part 1. Clinical study and determination of electrical field distribution in the numerical wound model. J. Bioelectrochem. Bioenerget. 1997; 43: 265–270.

5. J. Kerns, A. Fakhouri, H. Weinrib, J. Freeman. Electrical stimulation of nerve regeneration in the rat: The early effects evaluated by a vibrating probe and electron microscopy. J. Neurosci. 1991; 40: 93–107.

6. J. Pu, M. Zhao. Orientation and directed migration of cultured corneal epithelial cells in small electric fields are serum dependent. J. Cell Sci. 2005; 118: 1117–1128.

7. E. Wang, Y. Yin, M. Zhao, J. Forrester, C. McCaig. Physiological electric fields control the G1/S phase cell cycle checkpoint to inhibit endothelial cell proliferation. J. FASEB. 2003; 17: 458–460.

8. B. Garner, A. Georgevich, A. Hodgson, L. Liu, G. Wallace. Polypyrrole–heparin composites as stimulus-responsive substrates for endothelial cell growth. J. Biomed. Mater. Res. 1999; 44: 121–129.

9. M. Zhao, J. Forrester, C. McCaig. A small physiological electric field orients cell division. J. PNAS. 1999; 96: 4942–4946.

10. R. Williams, P. Doherty. A preliminary assessment of poly(pyrrole) in nerve guide studies. J. Mater. Sci. Mater. Med. 1994; 5: 429–433.

11. A. Akkouch, G. Shi, Z. Zhang, R. Mahmoud. Bioactivating electrically conducting polypyrrole with fibronectin and bovine serum albumin. J. Biomed. Mater. Res. 2010; 92A: 221-231.

12. J. Luis, E. Francesc, A. Elaine, O. Ramon, A. Carlos. Cellular adhesion, proliferation and viability on conducting polymer substrates. J. Macromol. Biosci. 2008; 8: 1144-1151.

13. S. Lakard, G. Herlem, N. Valles-Villareal, G. Michel, A. Propper, T. Gharbi, B. Fahys. Culture of neural cells on polymers coated surfaces for biosensor applications. J. Biosens. Bioelectron. 2005; 20: 1946-1954

14. J. Wong, R. Langer, D. Ingber. Electrically conducting polymers can noninvasively control the shape and growth of mammalian cells. J. Proc. Natl. Acad. Sci. 1994; 91: 3201–3204.

15. D. Ateh, H. Navsaria, P. Vadgama. Polypyrrole-based conducting polymers and interactions with biological tissues. J. Roy. Soc. Interface. 2006; 3: 741-752.

16. S. Abhisek, K. Prativa, P.L. Nayak. Use of biodegradable polymers for tissue engineering applications. J. Pop. Plast. Packaging. 2007; 52: 77-87.

17. A. Jamshid, O. Meng, F. Luca, R. Arthur, S. Amelia. Shielding effectiveness evaluation of metallized and polypyrrole-coated fabrics. J. Thermoplas. Compos. Mater. 2007; 20: 241-254.

18. G. Shi, M. Rouabhia, Z. Wang, L. Dao, Z. Zhang. A novel electrically conductive and biodegradable composite made of polypyrrole nanoparticles and polylactide. J. Biomater. 2004; 25: 2477–2488.

19. Z. Wang, R. Guidoin, Z. Zhang. A biodegradable electrical bioconductor made of polypyrrole nanoparticle/poly(D,L-lactide) composite: A preliminary in vitro biostability study. J. Biomed. Mater. Res. 2003; 66A: 738-746.

20. G. Shi, Z. Zhang, M. Rouabhia. The regulation of cell functions electrically using biodegradable polypyrrole-polylactide conductors. J. Biomater. 2008; 29: 3792-3798

21. S. Meng, .R. Mahmoud, G. Shi, Z. Zhang. Heparin dopant increases the electrical stability, cell adhesion, and growth of conducting polypyrrole/poly(L,L-lactide) composites. J. Biomed. Mater. Res. 2008; 87A: 332-344.

22. S. Yang, S. Zhang, F. Winnik, F. Mwale, Y. Gong. Group reorientation and migration of amphiphilic polymer bearing phosphorylcholine functionalities on surface of cellular membrane mimicking coating. J. Biomed. Mater. Res. 2008; 84A: 837-841.

TABLES:

1. Surface elemental composition and the C_{1s} components of the conductive membranes before and after cyclic voltammetric characterization

FIGURES:

1. Cyclic voltammetry of the PLLA/PPy composite membranes, showing the initial activation of electroactivity with the increasing number of scans from Scan001 to Scan100. The arrows show the forward and backward scans.

2. Cyclic voltammetry of the PLLA/PPy composite membranes, showing the slow deterioration of electroactivity with the increasing number of scans from Scan150 to Scan1000. The arrows show the forward and backward scans.

3. Cyclic voltammetry of the PLLA/PPy/HE composite membranes, showing the initial activation of electroactivity with the increasing number of scans from Scan001 to Scan150. The arrows show the forward and backward scans.

4. Cyclic voltammetry of the PLLA/PPy/HE composite membranes, showing the slow deterioration of electroactivity with the increasing number of scans from Scan200 to Scan1000. The arrows show the forward and backward scans.

5. The change of the maximum anodic current (switch point) of the composite membranes during CV scans, showing the initial rapid increase of electroactivity, the slow deterioration of electroactivity with repeated scans, and the superior stability of the PLLA/PPy/HE membranes. Dash lines represent the linear regression between 150 and 1000 scans for both membranes, and between 500 and 1000 scans for the PLLA/PPy/HE membrane.

6. The change of the maximum cathodic current (end point) of the composite membranes during CV scans, showing the initial rapid increase of electroactivity, the slow deterioration of electroactivity with repeated scans, and the superior stability of the PLLA/PPy/HE membranes. Dash lines represent the linear regression between 150 and 1000 scans for both membranes, and between 500 and 1000 scans for the PLLA/PPy/HE membrane.

7. The change of charge transfer with the increasing number of scans, showing similar trend as anodic and cathodic currents. Dash lines represent the linear regression

between 150 and 1000 scans for both membranes, and between 500 and 1000 scans for the PLLA/PPy/HE membrane.

8. The photomicrographs of scanning electron microscope of the PLLA/PPy (95:5) composite membranes before (A, C) and after (B, D) 1000 CV scans.

9. The ATR-FTIR spectra of the composite membranes before (b) and after (a) 1000 CV scans, and the spectra of the reference materials.

Table 1. Surface elemental composition and the C_{1s} components of the conductive membranes before and after cyclic voltammetric characterization

Samples	Elements (%)					C_{1s} (%)		
	C	O	N	Cl	Si	C-C-C	C-C-O	O-C=O
Composite with HE								
Before CV	76.2±2.7	21.1±2.5	1.2±0.2	0.1	1.5	74.2±2.5	18.5±2.9	7.3±3.6
After CV	72.7±0.5	25.6±0.7	0.6±0.2	0.1	1.3	70.0±2.3	17.9±1.9	12.4±0.6
Composite without HE								
Before CV	75.6±1.6	22.8±0.7	0.4±0.2	0.2	1.2	71.8±2.7	19.2±3.2	9.0±0.6
After CV	70.0±1.9	29.8±2.1	0.4±0.2	0.1	0.4	64.4±4	20.0±1.2	16.0±3.2
PPy on Pt electrode								
Before CV	73.2±1.3	13.1±2.7	13.2±2.2	<0.1	0.7	72.4±3.7	17.2±2.8	10.5±4.8
After CV	68.9±3.3	19.4±2.2	11.4±1.5	<0.1	0.4	61.2±0.6	24.7±1.2	13.5±0.7

48
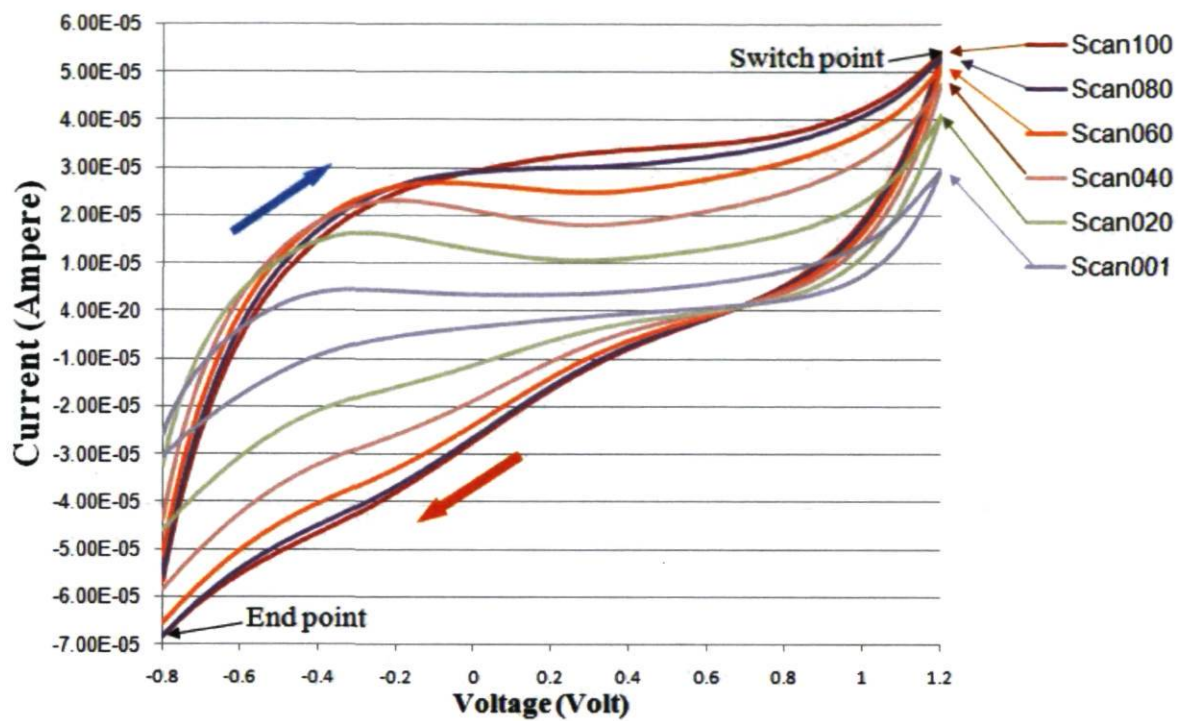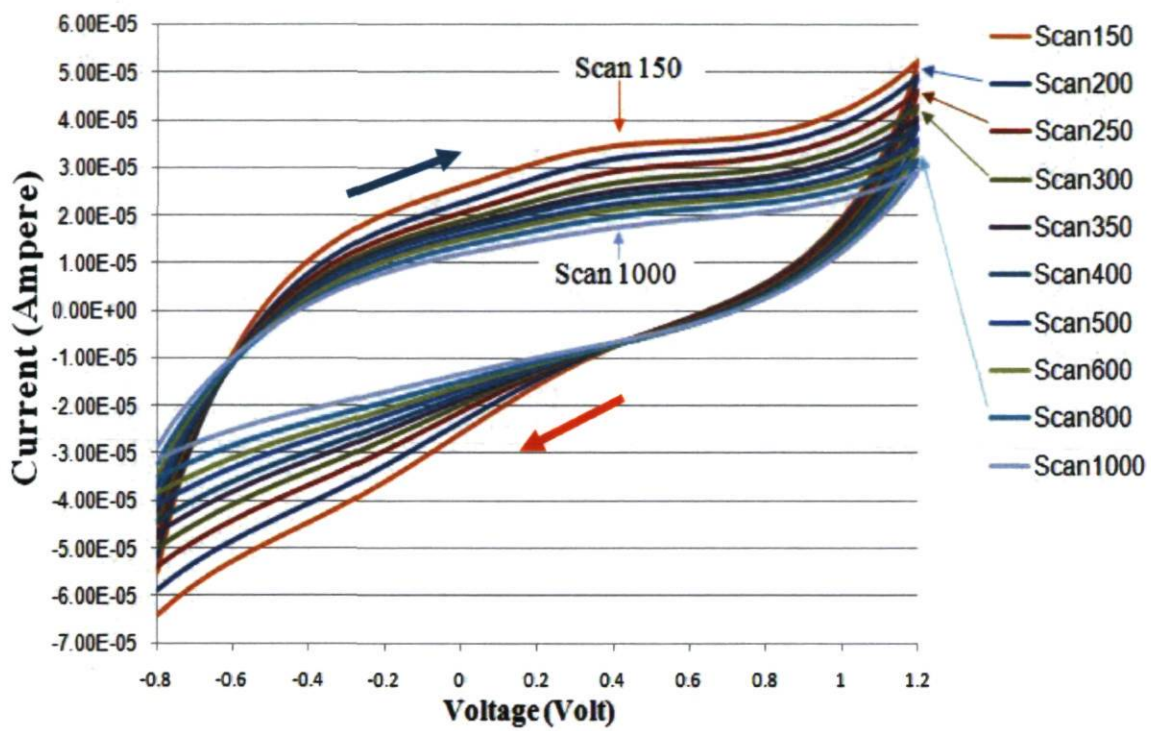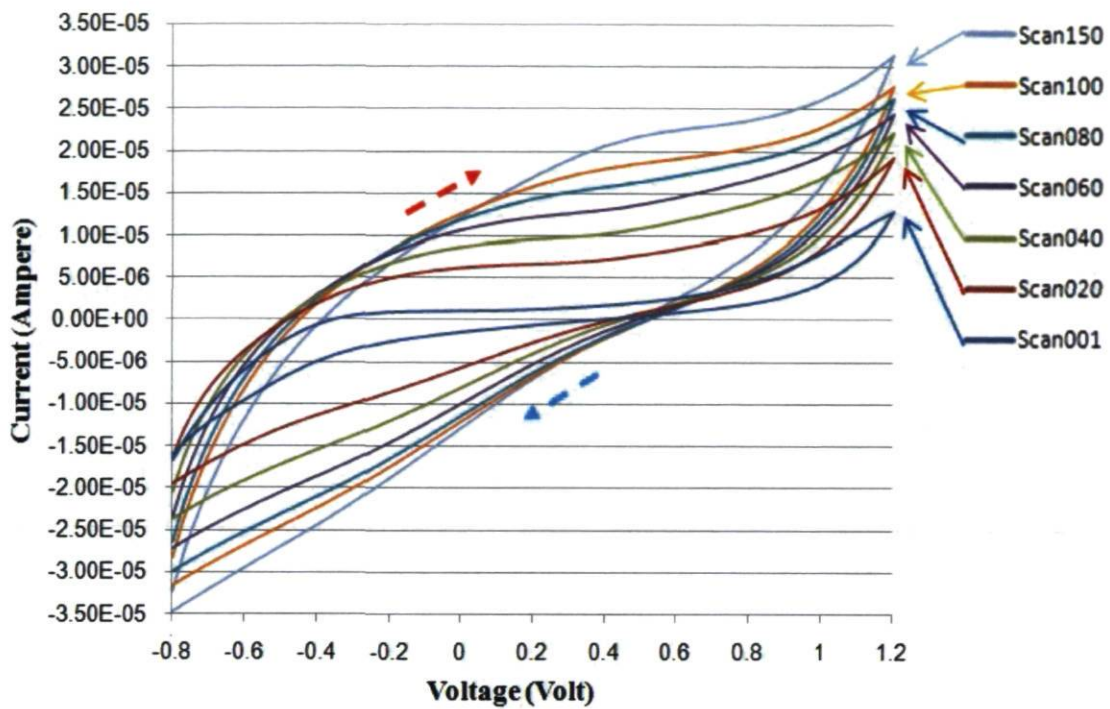
Figure 1
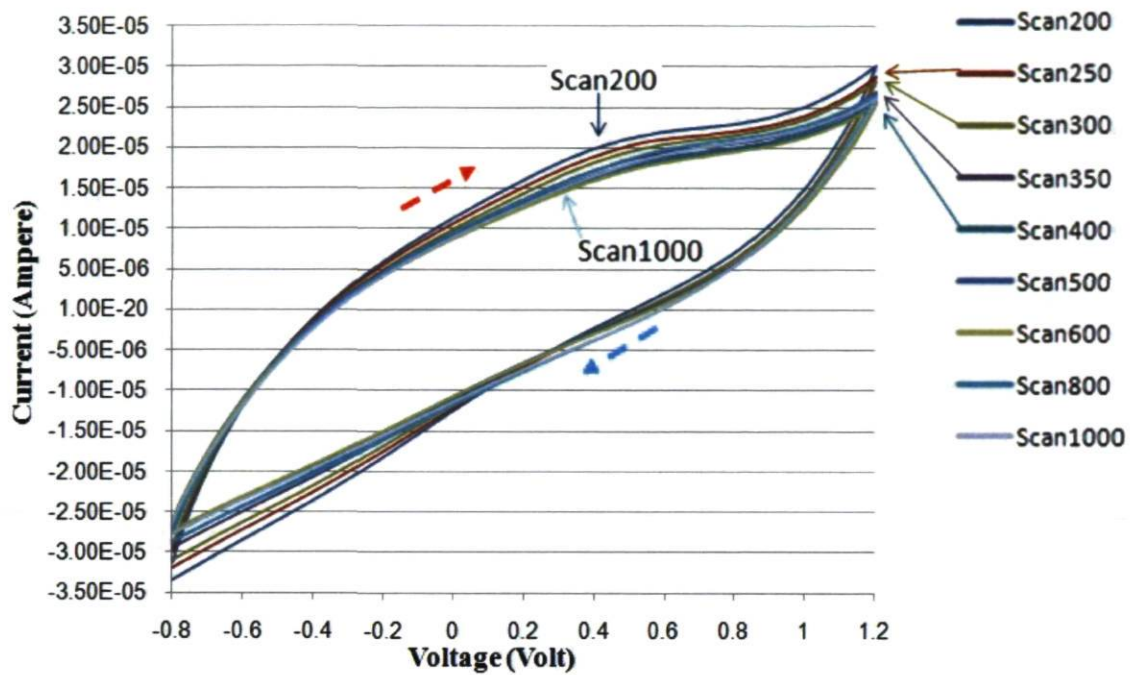
Figure 2
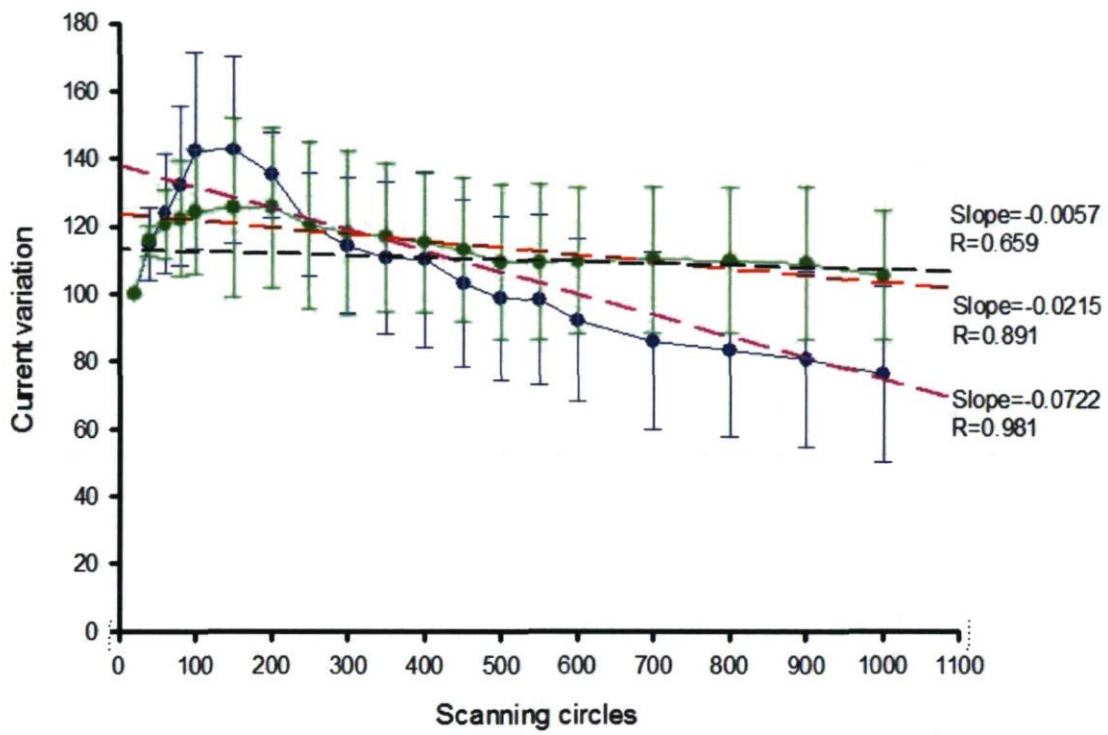
Figure 3
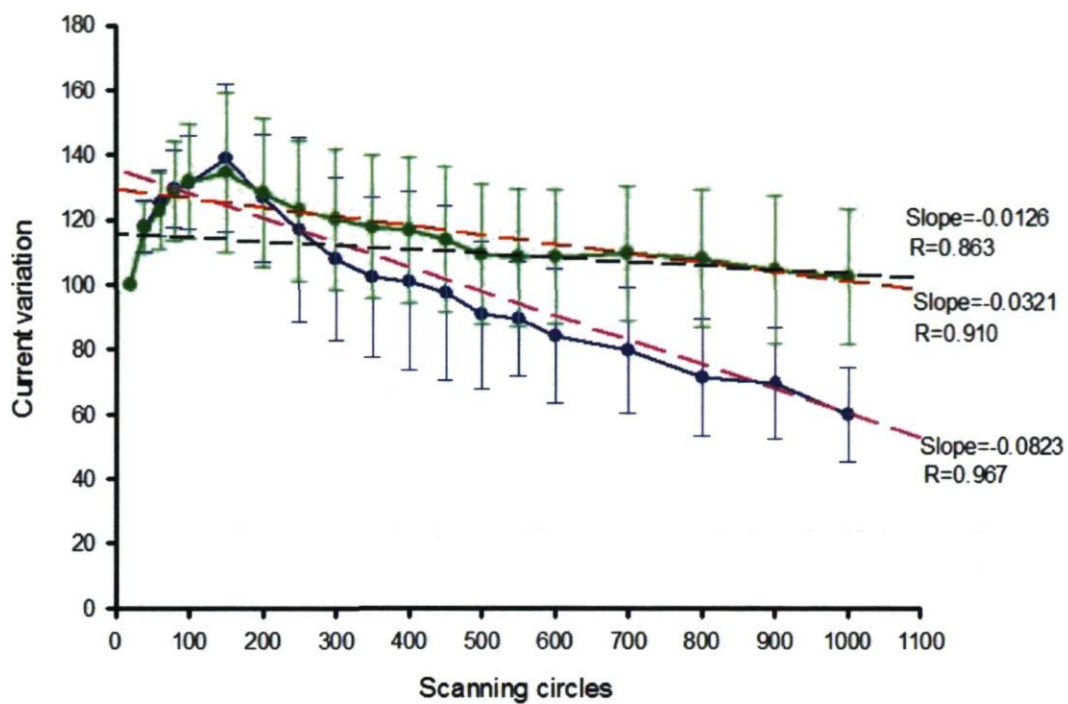
Figure 4
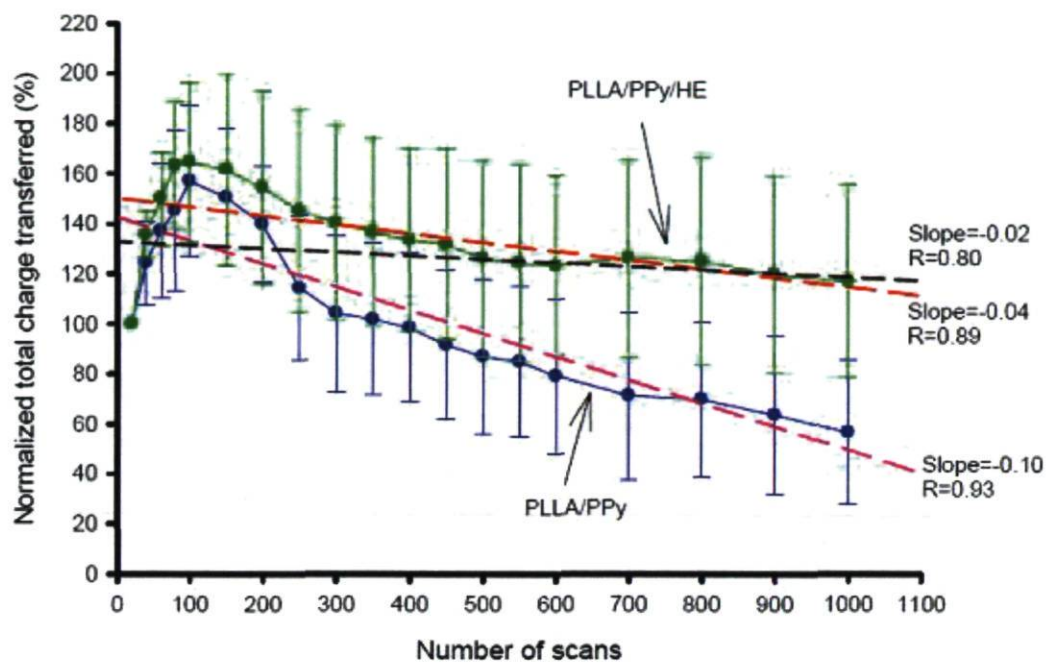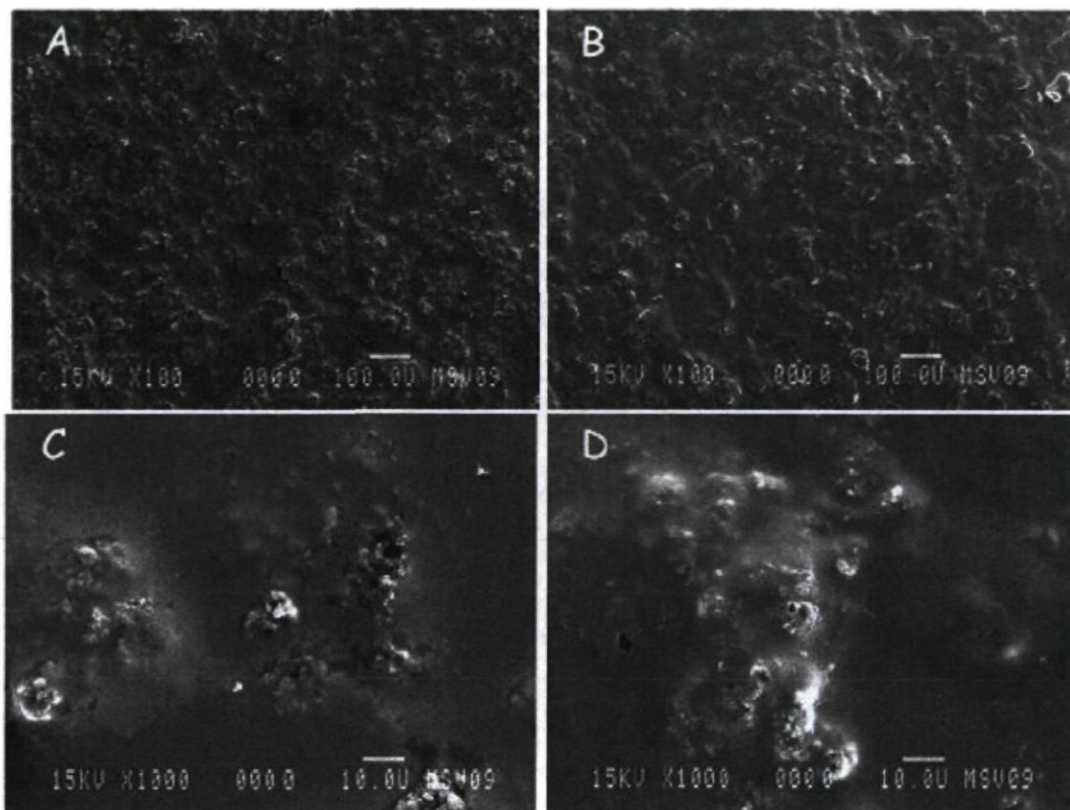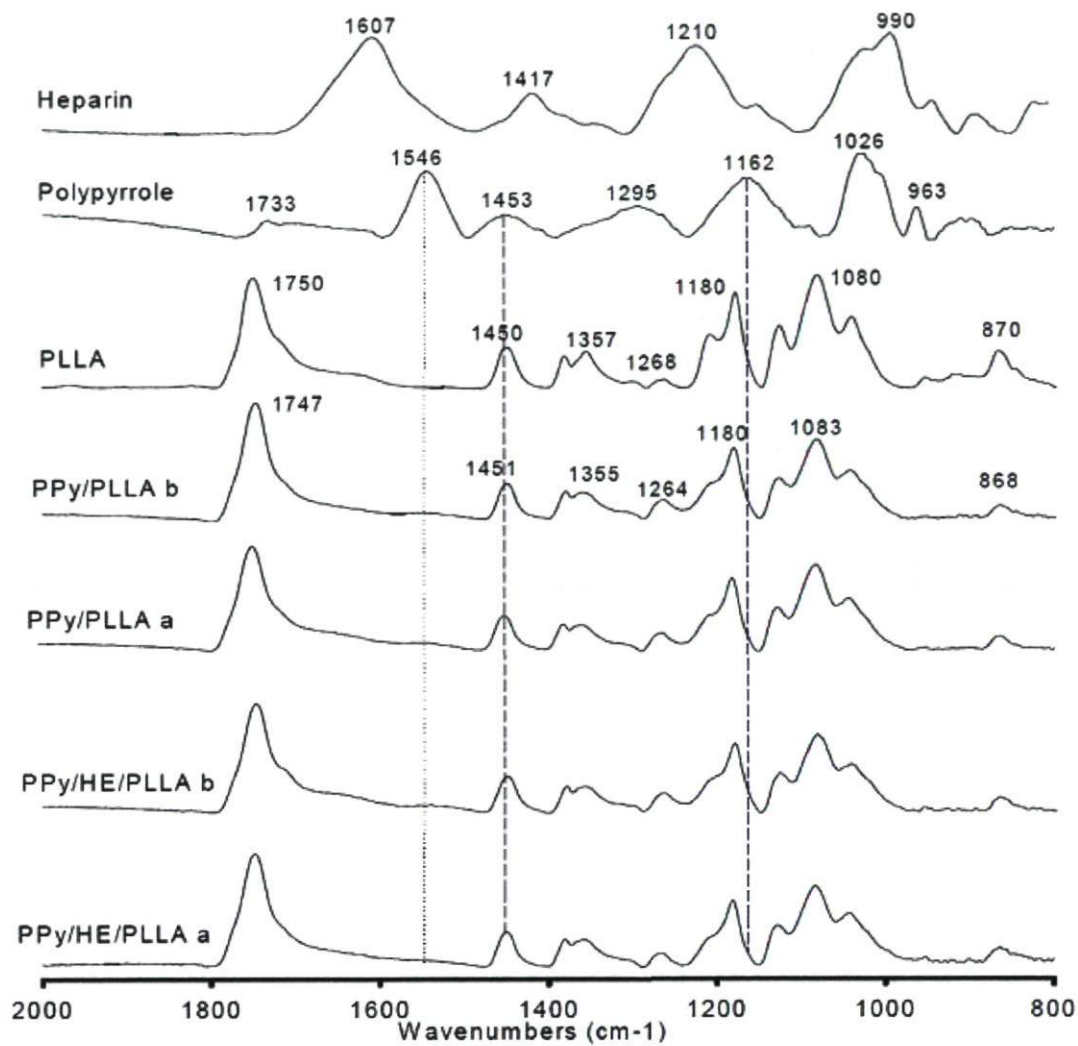
Figure 5

Figure 6

Figure 7

Figure 8

56

Figure 9

CHAPTER III

ELECTROCHEMICAL SYNTHESIS OF A FREE-STANDING POLYPYRROLE AND POLY(1-(2-CARBOXYETHYL)PYRROLE FILM AT THE AIR/LIQUID INTERFACE

SUMMARY

Thin flexible films of conductive polymers are useful in biosensors and flexible batteries. These films are typically prepared through electropolymerization on the surface of an electrode and are subsequently peeled off. We successfully synthesized a free-standing, thin flexible film made of PPy and poly(1-(2-carboxyethyl)pyrrole (PPyCOOH) at the air/liquid interface of a three-electrode system. XPS, ATR-FTIR and SEM were used to characterize the films. The important factors affecting the film growth such as the concentration of the monomers and electrolyte and the reaction voltage were discussed. High applied potential forced the flexible membrane growth large but over oxidation of the membrane. Hence, the current experiment set the reaction voltage at 1200mV. The result showed while the PPy films were overoxidized, both PPy and PPy/PPyCOOH copolymer films remained electrically active and stable up to 200 CV scans. And the membranes could growth up to with a diameter of 3.5mm and 1.5mm, respectively. Further experiments are required to increase film size and to investigate the unique surface morphology and associated mechanisms.

INTRODUCTION

Polypyrrole (PPy) has recently been extensively studied for biomedical applications (1). Our previous research centered on chemically synthesized conductive composites and electrically stimulated cell cultures (2-4). We know that PPy is often electrochemically synthesized because of several advantages such as *in situ* polymerization, high conductivity, and good electroactivity with various dopants including biomolecules. However, electrochemically produced PPy usually only contains a small percentage of other types of matrix polymers, resulting in a rigid product with limited secondary processability. Furthermore, synthesized PPy often strongly adheres to the electrode, making it difficult to peel off free-standing films.

We recently found that under specific conditions, PPy formed a free-standing film at the air-liquid (electrolyte) interface during electropolymerization. This phenomenon was reported by Song et al. in the late 1980s (5,6), and to our knowledge no further research in this area exists. The reported PPy films were very small, only approximately 90 microns in size. In light of the potential applications of conductive polymer films in areas such as sensor, light-emitting element, and flexible battery applications (7,8), we believe that this phenomenon warrants further exploration, as a free-standing PPy film with no supporting electrode represents a unique approach to electrochemically synthesize thin flexible conductive polymer films. Moreover, PPy film can be cut or rolled into different shapes.

This study focused on two objectives. The first objective was to increase the size of the free-standing PPy film, as only in the appropriate size can this film be processed and have any significant use in applications. The second objective was to explore the possibility of synthesizing a free-standing PPy and poly(1-(2-carboxyethyl)pyrrole (PPyCOOH) film. The rationale was to further chemically modify the PPy/PPyCOOH film with functional groups for potential biological applications.

MATERIALS AND METHODS

Synthesis of free-standing PPy film at the air/liquid interface

A three-electrode setup controlled by the Epsilon Electrochemical Workstation (Bioanalytical Systems Inc., West Lafayette, IN, US) was used to synthesize the PPy. A platinum (Pt) plate (Aldrich, 99.9%) 25 mm x 2 mm x 0.1 mm in size was used as the working electrode on which PPy was polymerized. Pt wire and Ag/AgCl electrode were used as the auxiliary and reference electrodes, respectively. To synthesize the PPy, 0.14 ml of distilled pyrrole monomers (final concentration 0.1 mol/L) and 0.3886 g of sodium p-toluenesulfonate (p-TSNa) (0.1 mol/L) were added in deionized water to prepare 20 ml of electrolyte under nitrogen protection. The experiment was carried out in potentiostatic mode at a room temperature of approximately $22^{\circ}C$. To synthesize the free-standing PPy films, the experiment was run at 1200 mV for 1200 seconds. For the regular PPy reference material, the experiment was run at 1000 mV for 500 seconds. The anodic current was determined at between 4 and 5 mA. Following synthesis, the PPy-growing Pt electrodes were cleaned repeatedly in distilled water and were dried in a vacuum oven prior to further analysis.

PPy was also synthesized according to Song et al. (6). For the working electrode, a Pt wire (Aldrich, 99.9% and 0.25 mm diameter) approximately 40 mm in length was bent to a 90° angle at 5 mm from one end and shaped in the form of an "L". The wire was then held perpendicular to the solution surface so that the 5-mm segment of the wire was just immersed under the air/liquid interface. A similar synthesis was performed as aforementioned, i.e., at a potentiostatic mode running at 1200 mV for 1200 seconds at room temperature and with a current ranging between 4 and 5 mA.

Synthesis of the free-standing PPy/PPyCOOH copolymer film

Electropolymerization was carried out using the same experimental setup as described above. The aqueous electrolyte in a cell vial contained 0.07 ml of distilled pyrrole

(0.05 mol/L), 0.14 g of 1 mM 1-(2-carboxyethyl)pyrrole (0.05 mol/L), 0.3886 g of p-TSNa (0.1 mol/L), and 20 ml of deionized water. Potentiostatic synthesis was performed at 1200 mV for 1000 seconds to obtain the free-standing film and at 1000 mV for 500 seconds to obtain regular PPy/PPyCOOH on an electrode. The anodic current was 4-5 mA.

For each synthetic experiment, before adding the monomers, the electrolyte was purged with nitrogen gas for 10 min prior to electropolymerization which was carried out under nitrogen gas protection.

Electrical characterization

Cyclic voltammetry was used to test the electroactivity and electrical stability of the synthesized PPy. The PPy films were removed from the electrode and immersed into the electrolyte held by Pt plates. The regular PPy deposited on the Pt electrode was used directly. An aqueous solution of p-TSNa (0.1 mol/L) was used as the electrolyte. Twenty millilitres of electrolyte in a cell vial were purged with nitrogen gas for 10 min before the experiment and were protected with nitrogen during the entire experiment. Epsilon potentiostat/galvanostat (BASi) equipment was used to control the three-electrode system with Ag/AgCl as the reference electrode and Pt wire as the auxiliary electrode. The experiment scan rate was 50 mV/s and the temperature was at room temperature at approximately 22°C.

Surface analysis

X-ray photoelectron spectroscopy (XPS)

The surface chemistry of the synthesized films was analyzed with a Perkin Elmer PHI 5600 X-ray photoelectron spectroscope (XPS) (Perkin Elmer, Eden Prairie, MN, USA). Surface elemental content was measured by means of a monochromatic aluminium source at 1486.6 eV and by high resolution spectra using a standard magnesium X-ray source at 1253.6 eV. The polymers deposited on the working electrode were also measured as

references. The take-off angle of the emitted photoelectrons was 45 degrees. The pass energy for the survey and high resolution scans was 187.9 eV and 5.85 eV, respectively. The vacuum in the sample chamber was maintained at 10^{-10} torr during analysis. Curve fitting for the high-resolution spectra was performed using the software provided by the instrument manufacturer. At least three specimens from each membrane were analyzed.

Attenuated total internal reflection Fourier transform infrared spectroscopy (ATR-FTIR)

The infrared absorption spectra of the specimens were collected with a Nicolet Magna-IR 550 spectrophotometer (Nicolet Instrument, Madison, WI, USA) in the ATR mode. The specimens were pressed against a single reflectance element and were scanned 150 times at a resolution of four wavenumbers per centimetre. Spectrum processing was performed using the software provided by the instrument manufacturer.

Scanning electron microscopy (SEM)

A JEOL JSM-35 scanning electron microscope (JEOL, Tokyo, Japan) was used to analyze the surface morphology of the synthesized PPy at an accelerating voltage of 15 kV. At least three specimens from each sample were observed. Prior to analysis, each sample was sputter coated with gold.

Statistical analysis

A t-test was used to analyze the statistic difference of the data. The difference between the control and test groups was considered significant when $p < 0.05$.

RESULTS

Macroscopic morphology of the synthesized PPy

Figure 1 shows the macroscopic images of the PPy on the electrode as synthesized, taken with an ordinary digital camera (8 M pixels). Figure 1A shows a free-standing PPy film formed around the Pt plate at the air/liquid interface. Synthesized at 1200 mV for 1200 sec, the flexible film had a diameter of 3.2-3.5 mm, which was fairly circular and symmetrical to the electrode. As a reference of Figure 1A, Figure 1B recorded the PPy synthesized at 1000 mV for 1200 sec on a similar electrode, showing no PPy film at the the air/liquid interface. Figure 1C is the PPy film formed on the Pt wire at the air/liquid interface, using 1000 mV and 1200 sec as described in reference 6. The film, which was separated from the Pt wire, grew less than 1 mm from the electrode. Figure 1D shows the free-standing PPy/PPyCOOH copolymer film formed at the air/liquid interface of a Pt plate. The size of the film was slightly smaller than that of the PPy film (Fig. 1A) formed under the same synthesis conditions.

Electrical characterization

Figure 2 shows the representative CV scans of the free-standing PPy films from -600 to 400 mV. While the PPy film was electrically active by showing a fair amount of anodic current and charge transfer, no obvious oxidation and reduction peaks were observed on the scanning curves. The deflections at approximately 60 mV in the forward scans and at approximately -200 mV in the backward scans did indicate some redox activities. As it shows, with the increasing number of cycles, the decrease of anodic current as well as the integrated charge (area within the CV curve) was very small. In comparison, the PPy/PPyCOOH film recorded distinct redox behaviours (Fig. 3), with oxidation and reduction peaks at 150 mV and -150 mV, respectively. However, unlike the relatively stable PPy film, the integrated charge transfer of the PPy/PPyCOOH films deteriorated with the increasing number of scans, accompanied by a slight shift of the redox peaks toward low potential direction.

Figures 4 and Figure 5 present the CV curves of the regular PPy (Fig. 4) and PPyCOOH (Fig. 5) deposited on the working electrode. Both polymers revealed typical redox behaviours, with the PPy/PPyCOOH recording an oxidation peak at approximately 0 mV which was much higher than that of the PPy at -250 mV. However, their reduction peaks were quite similarly positioned between -820 mV for the PPy and -850 mV for the PPy/PPyCOOH. With the increasing number of scans, the separation of the oxidation and reduction peaks of both polymers became narrowed by shifting inward, although the changes were minimal after 40 scans for the PPy and after 20 scans for the PPy/PPyCOOH, showing very good stability.

Surface analysis

X-ray photoelectron spectroscopy

XPS recorded (Table 1) a similar surface elemental composition on both sides of the PPy films. The curve fitting results of the C_{1s} spectra also revealed a comparable oxidative status on both sides of the film. The regular PPy on the Pt electrode showed higher N and lower O than the PPy flexible film did. The C_{1s} of the regular PPy also showed less oxidized carbons (CCO and OCO) compared to the PPy flexible film (28% versus 42%), indicating less oxidation in the regular PPy than in the PPy films.

Because the regular PPy was synthesized at a lower potential, there was lower oxygen content and higher nitrogen content. Following CV characterization, the oxygen content increased 48%, accompanied by the increase of C-O and OC=O. Furthermore, the surface elemental and high resolution scans of the PPy/PPyCOOH on the Pt electrode both proved that the PPy and the PPyCOOH had polymerized together.

ATR-FTIR spectroscopy

Figure 6 shows the infrared spectra of the free-standing PPy films and their regular forms, i.e., polymer deposited directly on the electrode. Compared to the spectrum of the regular PPy, the decrease of 1546 cm^{-1} and the shift at 1162 cm^{-1} and 1026 cm^{-1} of the PPy film confirmed the oxidation during synthesis. For the PPy/PPyCOOH film, the characteristic carbonyl absorption at 1700 cm^{-1} clearly revealed the presence of O-C=O in the copolymer.

Scanning electron microscopy

Figures 7A and 7B show the regular PPy deposited on the working electrode at magnifications of x200 and x1000. The low magnification image (A) shows that the smooth surface of the Pt electrode was fully covered by a layer of PPy with uniformly distributed particles. At high magnification (B), these particles displayed the typical cauliflower morphology of granulated PPy. Figures 7C and 7D present the surface morphology of the free-standing PPy films, which was relatively smooth with no granulation. Note the straight lines radiating from the center of the circular film, or from where the Pt working electrode was located (Fig. 7C, right). The surface morphology of the PPy/PPyCOOH copolymer in the form of either film or deposited on the electrode was similar to that of the PPy and therefore is not shown.

DISCUSSION

Free-standing conductive polymer films have the potential to be used in biosensors (11) or flexible rechargeable batteries (12). Since 1979, when Diaz et al. (13) first electrochemically synthesized free-standing PPy film, its electrochemical preparation has been carried out exclusively on a flat working electrode, followed by a peeling off of the film from the electrode. The resurgence of research on free-standing PPy films in recent

66

years remains focused on this technique (14,15). In 1988, Song et al. (5,6) found that free-standing PPy film could take place at the air/liquid interface, yet were only able to grow 90 microns which was too small for any meaningful characterization and application.

In the present work, various electrochemical techniques and experimental parameters were tested to produce a relatively large PPy film of nearly 25 mm^2. The thickness of the film was estimated to be less than 10 microns. Despite the small size of the PPy film, it is large enough to undergo typical analytical characterizations and also likely has sufficient surface area for sensoring applications. This study also demonstrates that both free-standing PPy film and free-standing PPy copolymer film (PPy/PPyCOOH) can be prepared through this interfacial polymerization technique. The surface carbonyl groups allow for further chemical modifications, thereby leading the way for grafting sensoring molecules.

Compared to the films polymerized on the electrode surface, the films polymerized at the air/liquid interface displayed several characteristics. The oxidation potential of both the PPy and PPy/PPyCOOH films was higher than that of their counterparts formed directly on the electrode, thus indicating a possible over-oxidation of the films. XPS data certainly support this possibility by revealing the high percentage of oxygen, C-O, and O-C=O components in the PPy film which showed the lowest level of electroactivity. The oxygen content and percentage of C-O and O-C=O in the PPy/PPyCOOH film was, however, similar to that in the regular PPy and PPy/PPyCOOH. Consequently, the PPy/PPyCOOH films recorded good electroactivity which was only slightly lower than that of the regular PPy/PPyCOOH film deposited on the electrode.

Why the PPy/PPyCOOH film showed greater electroactivity remains unclear. The presence of PPyCOOH in the copolymer was confirmed by infrared (Fig. 6); however, its role in the copolymerization process must be elucidated. For example, the PPy/PPyCOOH

appeared not to be over-oxidized even though it was synthesized under 1200 mV for 1200 seconds with the same potential and duration as that used to synthesize the PPy films.

Another clear feature of the interfacially synthesized films was their unique surface morphology. Markedly different from the traditional cauliflower-like particle topography, the interfacially synthesized films showed no such granulation but rather a smooth wave-like appearance. The regularly separated radial lines and the fine pattern along these lines merit further research on the mechanism of polymer growth and the effect of electrical field. These studies will hopefully provide further knowledge on how to produce larger free-standing films with improved electroactivity based on this interfacial polymerization technique.

Several experimental parameters were tested in this study to maximize film size. Potentiostatic, galvanostatic, and cyclic voltammetric methods all generated flexible free-standing films at the air/liquid interface, which means that the deposition of PPy and most likely other types of conductive polymers at the air/liquid interface is a common phenomenon under certain conditions. The potentiostatic and galvanostatic methods were better than was CV in terms of obtaining large-sized films. On the other hand, the free-standing PPy film achieved greater electroactivity when synthesized by CV than by the other two methods, most likely because during the same polymerization time, the potentiostatic and galvanostatic methods represented a longer oxidation period compared to the CV method, which probably caused more extensive oxidation.

Three main factors influence film formation at the air/liquid interface. The first is the contact area of the electrode immersed in electrolyte. The contact area of the electrode at the air/liquid interface should increase and the electrode area under the electrolyte should decrease. Another factor is electrolyte and monomer concentration. High concentration has a positive effect on the film growth. If the concentration of the electrolyte or the monomers

is too low, it is impossible to form a film at the air/liquid interface. The impact on film formation is most significant when the concentrations are increased to an optimal level. After that, any further increase of concentration will have less impact. The most important factor, however, is the applied electrical potential. At moderate potential, such as from 600 mV to 800 mV, the polymers only deposit on the electrode surface. In this study, an oxidation potential of 1200 mV was deemed to be optimal to grow large free-standing films at the air/liquid interface.

According to our visual observation during the reaction, the PPy first rapidly deposited on the working electrode. The film formed at the air/liquid interface and its growth was visible to the naked eye. While the initial growth was very fast, the growth speed decreased as the film diameter increased. This was probably because of the increasing resistance which caused the lowering of the oxidation potential at the edge of the film as the latter became larger. The average growth speed of the PPy film was roughly calculated as 3×10^{-3} mm/second at 1200 mV, however this value was influenced by other parameters.

CONCLUSIONS

This study confirms that free-standing PPy and PPy/PPyCOOH copolymer film can be formed at the air/liquid interface without metallic support. The interfacially synthesized films were electrically active, displayed stable CV behaviours up to 200 scans, and had smooth surface morphology with specific features. The films were likely over-oxidized because of the high oxidation potential at electropolymerization. This study proposes a new technique to electrochemically generate flexible free-standing conductive polymer films.

REFERENCES

1. D. Ateh, H. Navsaria, P. Vadgama. Polypyrrole-based conducting polymers and interactions with biological tissues. J. R. Soc. Interface. 2006; 3: 741–752.

2. Z. Wang, R. Guidoin, Z. Zhang, A biodegradable electrical bioconductor made of polypyrrole nanoparticle/poly(D,L-lactide) composite:A preliminary in vitro biostability study, J. Biomed. Mater. Res. 2003; 66A: 738-746.

3. G. Shi, Z. Zhang, M. Rouabhia, The regulation of cell functions electrically using biodegradable polypyrrole-polylactide conductors, J. Biomater. 2008; 29: 3792-3798.

4. S. Meng, .R. Mahmoud, G. Shi, Z. Zhang, Heparin dopant increases the electrical stability, cell adhesion, and growth of conducting polypyrrole/poly(L,L-lactide) composites, J. Biomed. Mater. Res. 2008; 87A: 332-344.

5. E.H. Song, W. Paik, J. Chon, J. Bull. Electrochemical Polymerization of Pyrrole in Aqueous Solutions: 1. Comparison of Solution-Surface-Growth and In-Solution-Growth Methods. J. Kor. Chem. Soc. 1988; 9: 413-414.

6. E.H. Song, W. Paik, J. Chon, J. Bull. Electrochemical Polymerization of Pyrrole in Aqueous Solutions: 2. Growth Kinetics of Polypyrrole p-toluenesulfonate Film. J. Kor. Chem. Soc. 1990; 11: 41-44.

7. Marek Trojanowicz. Application of Conducting Polymers in Chemical Analysis. J. Microchim. Acta. 2003; 143: 75–91.

8. C. Wang, G. Tsekouras, P. Wagner, S. Gambhir, C. Too, D. Officer, G. Wallace. Functionalised polyterthiophenes as anode materials in polymer/polymer batteries. J. Synth. Met. 2010; 160: 76-82.

9. A. Nath. A study of polypyrrole films formed at the liquid/vapor interface. J. Electroanal. Chem. 2004; 571: 9-14

10. S. David. Dopant Exchange in Conducting Polypyrrole Films. J. Polym. Int. 1992; 27: 231-235

11. T. Ahuja, I. Mir, D. Kumar, Rajesh. Biomolecular immobilization on conducting polymers for biosensing applications. J. Biomater. 2007; 28: 791-805.

12. T. Otero, I. Cantero. Conducting polymers as positive electrodes in rechargeable lithium-ion batteries. J. Power Sources. 1999; 81-82: 838-841.

13. A. Diaz, K. Kanazawa, G. Gardini. Electrochemical polymerization of pyrrole. J. Chem. Soc., Chem. Commun. 1979; 14: 635–636.

14. R. Chepuri. D. Rao. Trivedi. A novel one-pot synthesis of free-standing Pd–PPy films: Observation of enhanced catalytic effect by Pd-Ppy layers. J. Catal. Commun. 2006; 7: 662–668.

15. J. Wang, S. Chou, J. Chen, S. Chew, G. Wang, K. Konstantinov, J. Wu, S. Dou, H. Liu. Paper-like free-standing polypyrrole and polypyrrole–LiFePO4 composite films for flexible and bendable rechargeable battery. J. Electrochem. Commun. 2008; 10: 1781–1784.

TABLES:

1. Surface chemistry of the free-standing PPy films before and after CV scan, and the compared surface chemistry of the PPy/PPyCOOH and the PPy deposited on the Pt surface, as measured by XPS.

FIGURES:

1. Macroscopic images of the free-standing PPy film (A), the PPy deposited on the Pt plate (B), the very small PPy film on the Pt wire (C), and the free-standing PPy/PPyCOOH film on the Pt plate (D), showing the significantly larger film size compared to that synthesized according to literature #6 (C).

2. CV scans of the free-standing PPy film generated electrochemically at the air/liquid interface, showing an electrically active film and the unclear redox behaviour of the PPy film.

3. CV scans of the free-standing PPy/PPyCOOH film generated electrochemically at the air/liquid interface, showing the clear redox behaviour of the copolymer film.

4. CV scans of the regular PPy deposited directly on the Pt electrode, showing the typical redox behaviour and high electroactivity.

5. CV scans of the regular PPy/PPyCOOH deposited directly on the Pt electrode, showing the typical redox behaviour and high electroactivity.

6. ATR-FTIR spectra of the free-standing PPy film, regular PPy, and the PPy/PPyCOOH copolymer film, showing the oxidation of the PPy film and the presence of PPyCOOH in the PPy/PPyCOOH copolymer.

7. SEM photomicrographs of regular PPy deposited on the working electrode (A and B). Note the difference between the typical "cauliflower" morphology of the PPy and the morphology of the PPy film deposited at the air/liquid interface (C and D).

Table 1. Surface chemistry of the free-standing PPy films before and after CV scan, and the compared surface chemistry of the PPy/PPyCOOH and the PPy deposited on the Pt surface, as measured by XPS.

| Samples	Elements (%)					C$_{1s}$ (%)		
	C	O	N	S	Si	C-C-C	C-C-O	O-C=O
Free-standing PPy film								
Air-facing side	77.8±2.1	17.2±1.3	6.8±1.3	0.3	<0.1	57.3±4.3	34.7±3.2	8±1.0
Solution-facing side	76.3±2.7	17.7±1.4	7.8±1.5	0.3	<0.1	58.6±3.6	35.4±2.3	6.2±1.4
PPy on Pt electrode (PPy film forming electrode)	72.7±2.3	16.1±1.2	9.6±1.0	0.8	0.8	70.4±3.0	18.2±1.2	11.5±1.5
Regular PPy on Pt electrode without membrane								
Before CV	73.2±1.3	13.1±2.7	13.2±2.2	0.4	0.7	72.4±3.7	17.2±2.8	10.5±4.8
After CV	68.9±3.3	19.4±2.2	11.4±1.5	0.2	0.4	61.2±0.6	24.7±1.2	13.5±0.7
PPy/PPyCOOH on Pt electrode	74.6±1.2	15±0.6	10±0.5	<0.1	0.4	76.3±1.8	14.7±1.4	9±1.8

Figure 1
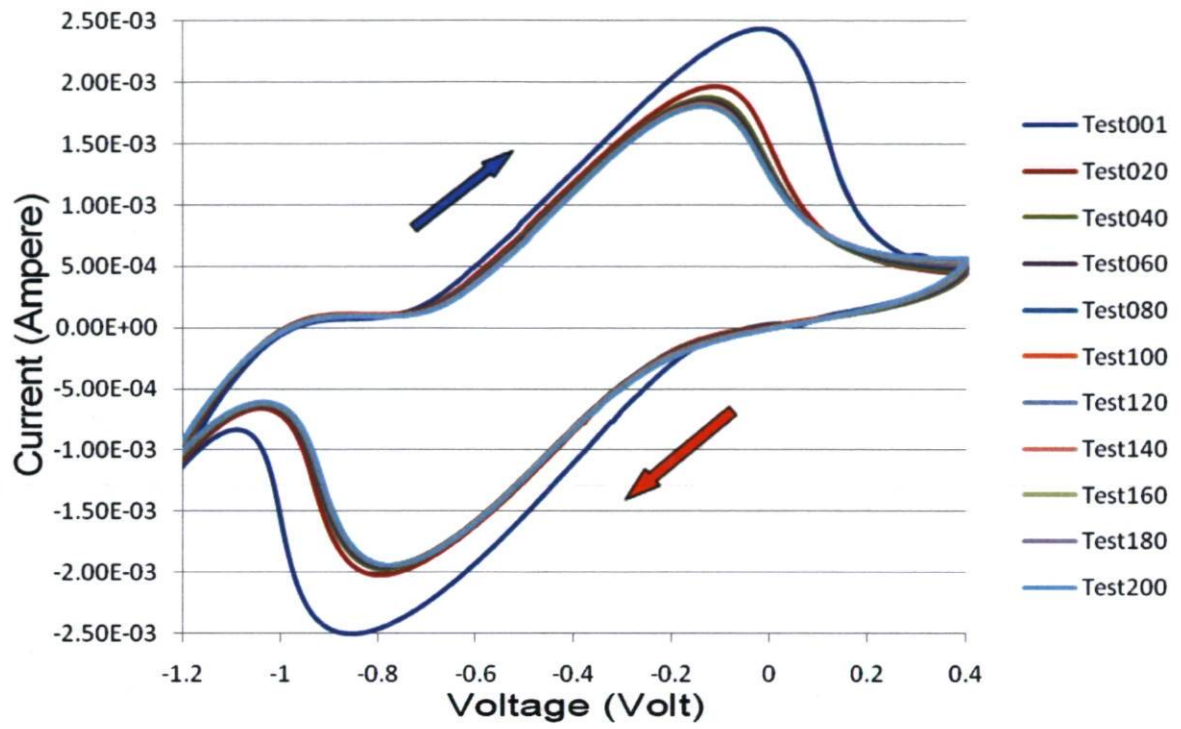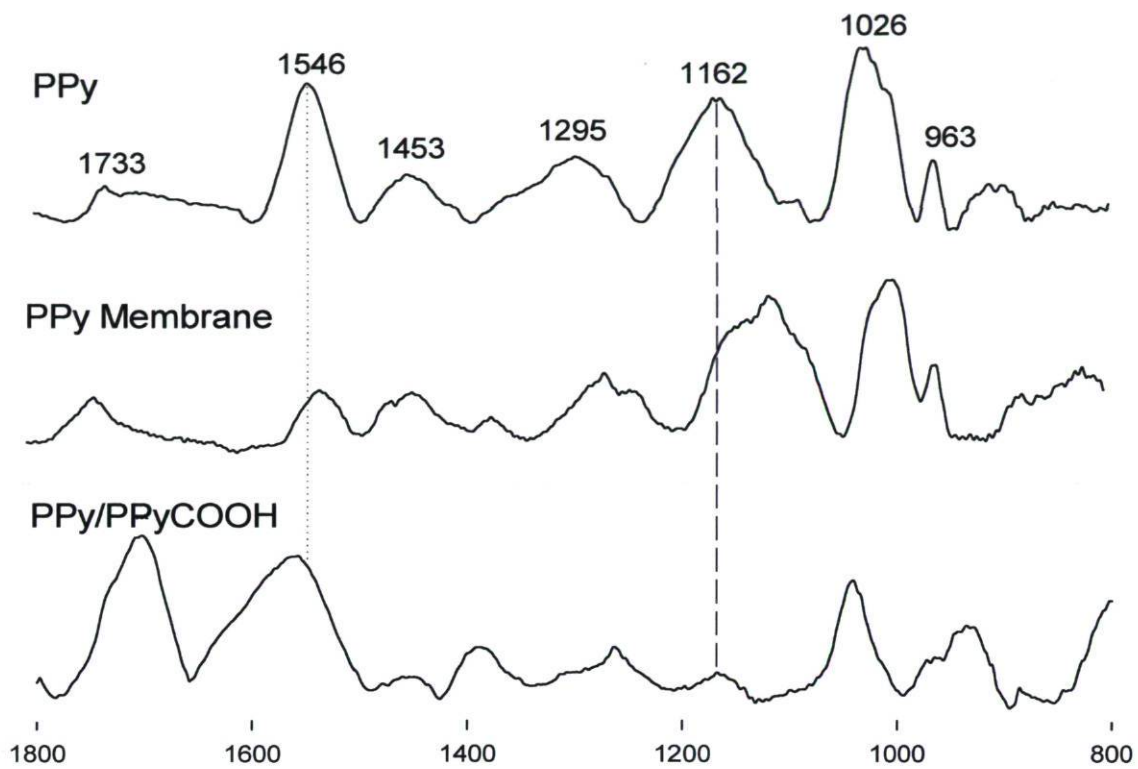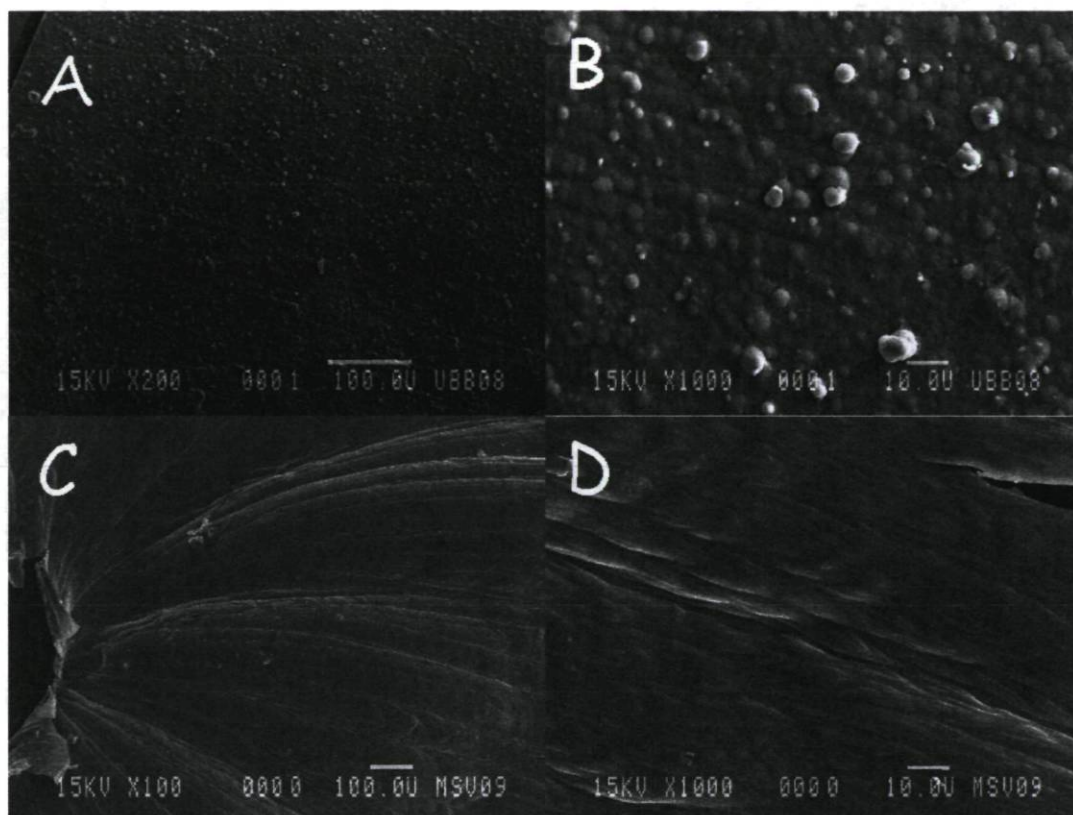
Figure 2

Figure 3

Figure 4

Figure 5

79
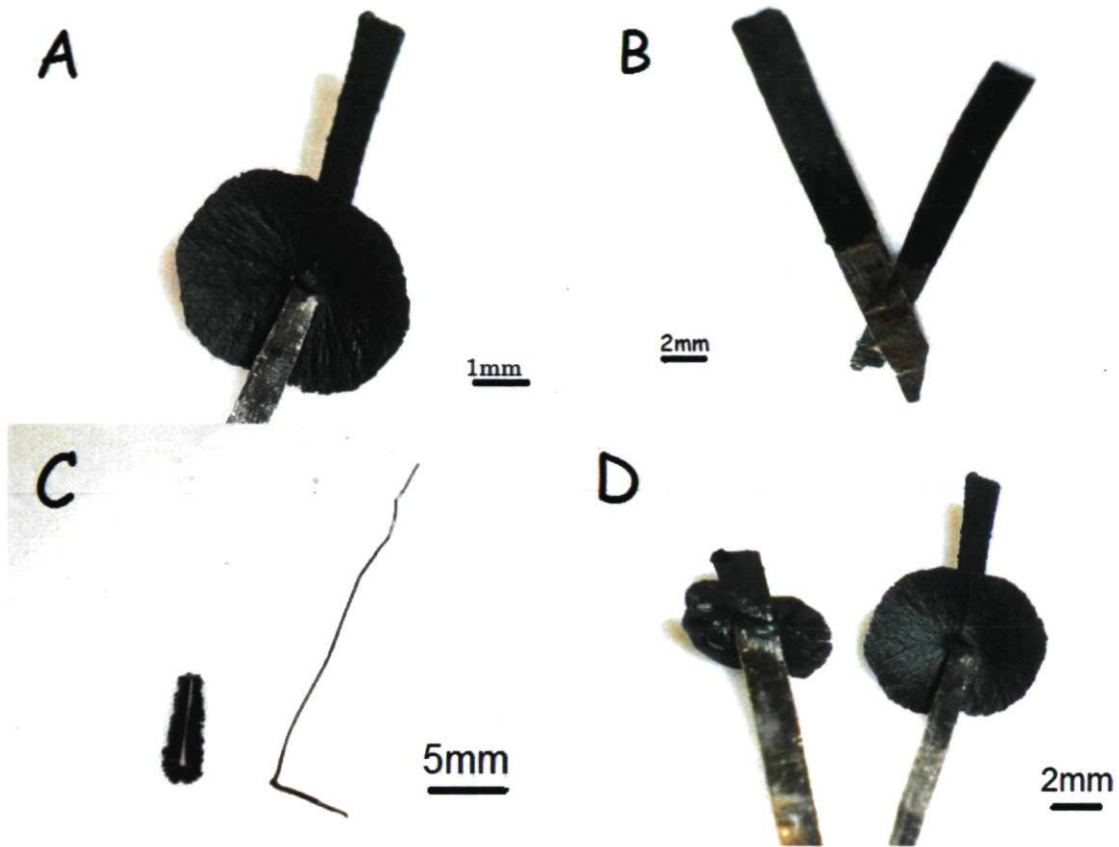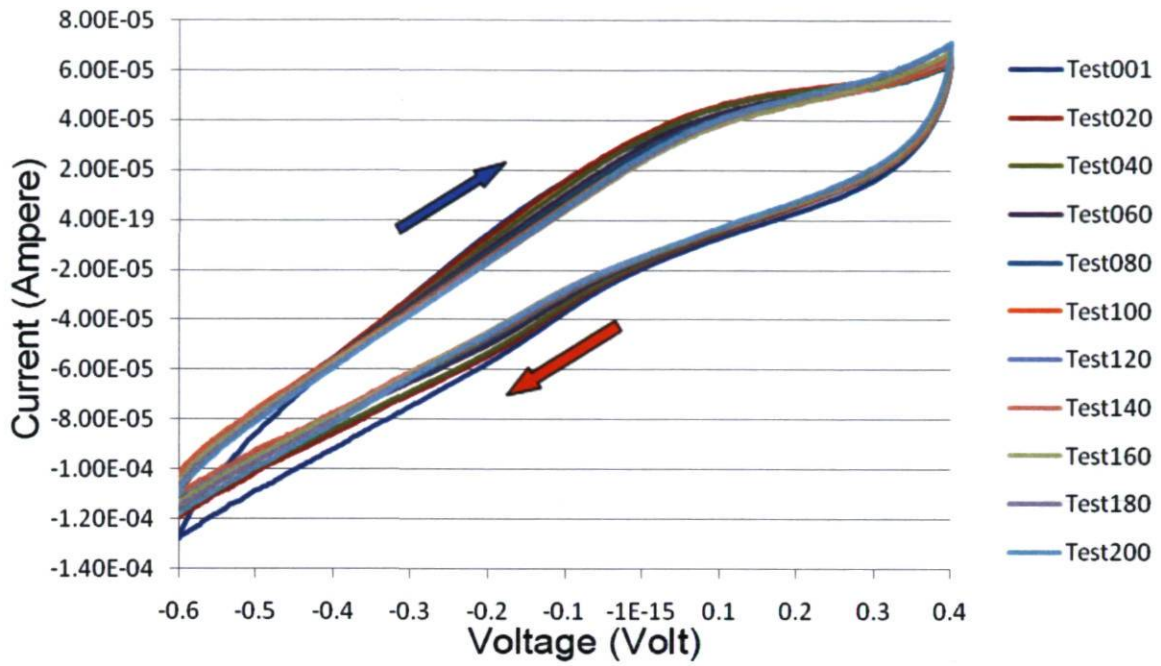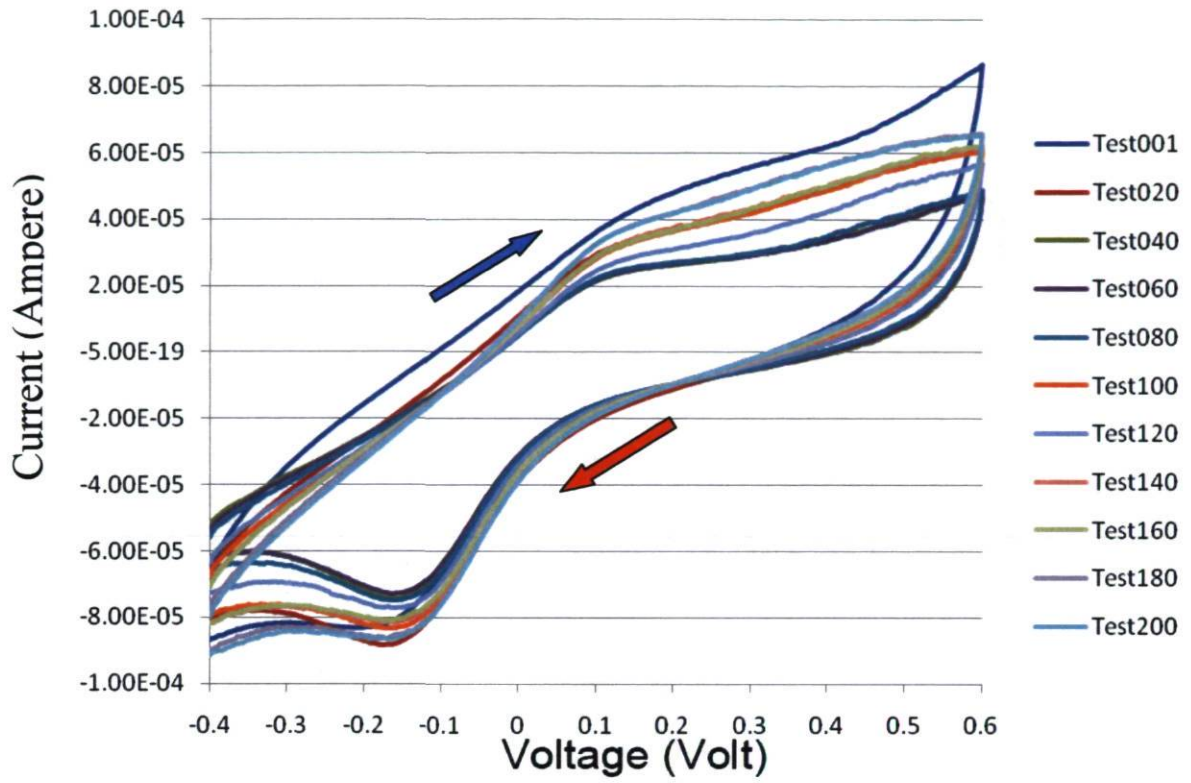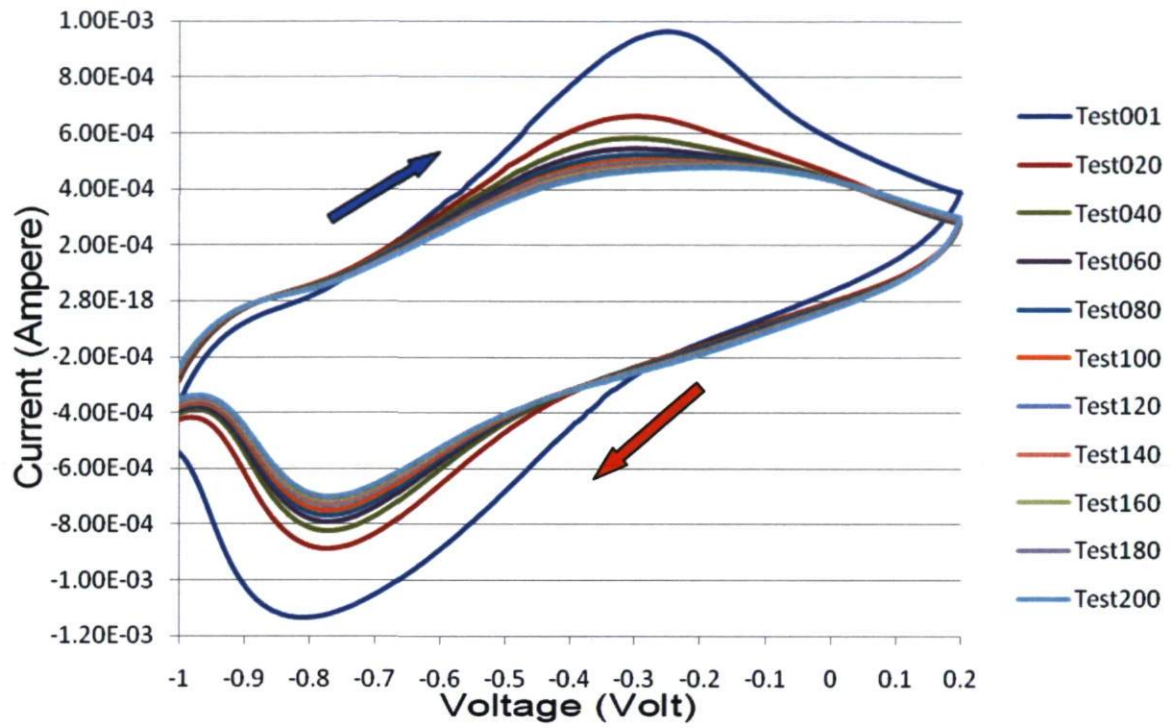
Figure 6

Figure 7

GENERAL CONCLUSIONS

This thesis investigated the chemical and electrochemical properties of PLLA/PPy/HE composite membranes and explored a unique approach to electrochemically generate free-standing conductive polymer films.

The electroactivity and electrical stability of the PPy/PLLA composite membranes with or without heparin were investigated by means of the cyclic voltammetry method. With only 5% PPy in the bulk system, the membranes displayed electroactivity and redox characteristics. During 1000 CV scans, the electroactivity of the composite membranes showed a period of initial activation, followed by a relatively stable period and finally a slow deterioration process. This behavior was controlled by the exchange of dopant between the PPy composite and the electrolyte and by the progressive oxidation of the PPy. The PLLA/PPy/HE membranes demonstrated superior electrical stability over the PLLA/PPy membranes and were estimated to last for 10,000 redox cycles. This study proves that the composite made of heparin-doped PPy was electrically stable and may be used for multiple electrical stimulations.

The electrochemical growth of free-standing conductive polymer film on the surface of an electrolyte is innovative. Compared to traditional electropolymerization on the surface of a flat electrode, the resulting conducting film generated by this air/liquid interfacial polymerization technique does not display the classic granulated appearance but rather smooth radial patterns. Furthermore, it does not need to be peeled from any substrate. The PPy/PPyCOOH copolymer film had high electroactivity and showed clear redox behaviour. In contrast, the PPy film showed no clear redox behaviour and was over-oxidized. The films appeared flexible and very thin. This approach therefore provides a promising alternative to currently available methods for the preparation of free-standing conductive polymer films.

PERSPECTIVES

PLLA/PPy/HE composites are intended for biomedical applications, and for this reason the electroactivity of this material should be tested in biological medium containing multiple ions and proteins. Protein absorption and potential denaturation should also be investigated along with other types of biological anions as the dopant.

The size of the free-standing film remains small and therefore further experimentation is required to make large films. The over-oxidation of the PPy film must also be addressed in order to increase its electroactivity. The unique appearance of the films calls for detailed physical and chemical analyses, which may lead to novel applications. Further surface modification of the PPy/PPyCOOH film with functional molecules is also very promising.

LIST OF PUBLICATIONS

1. Linli Zhang, Shiyun Meng, Ze Zhang. Electroactivity and stability of the polylactide/polypyrrole composites, submitted to the Journal of Biomaterials Science: Polymer Edition (Accepted).

2. Linli Zhang Ze Zhang. Electrochemical synthesis of free-standing polypyrrole and poly(1-(2-carboxyethyl)pyrrole film at air/liquid interface. (Under preparation).